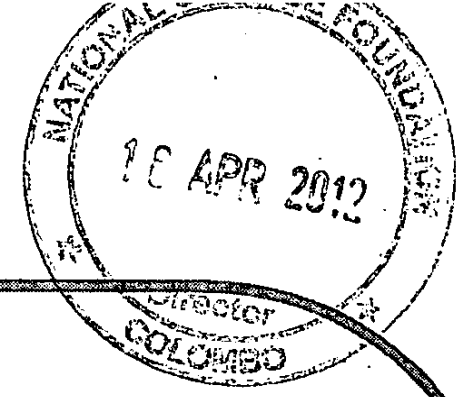


FR 1630



National Science Foundation, Sri Lanka

Final report

i) Grant Number:

RG/2007/FR/07

ii) Title of the Project:

Characterization of nanostructured polymer /
fullerene solar cells under direct sun light

iii) Total allocation of funds : Rs. 1,896,333.00

iv) Period : January 2008 – April 2012

v) Principle Investigator :

Prof. P. Ravirajan, Department of Physics

University of Jaffna

National Science Foundation, Sri Lanka

Characterization of Nanostructured Polymer: Fullerene Solar Cells

Final report

Section 1

Information regarding Project/ Project Personal:

- i) Grant Number
RG/2007/FR/07
- ii) Title of the Project
Characterization of nanostructured polymer: fullerene solar cells under direct sun light
- iii) Principle Investigator
Prof. P. Ravirajan
- iv) Co-Investigator

- v) Institute(s) where research was being carried out
Department of Physics, University of Jaffna
- vi) Date of award
January 2008
- vii) Date of completion of project
April 2012 30/6/2011
- viii) Total allocation of funds (Rs)
Rs. 1,896,333.00
- ix) Total Spent (Rs)

Personal	898,333.33
Miscellaneous	2,000.00
Glovebox	777,038.13
Custom duty & clearing charges	347,071.00
Total	2,024,442.46
- x) Number of Research Students employed
One (01)
- xi) Post graduate degree completed with dates
Submitted thesis in February 2012

- xii) Number of Technical Assistants and/or labourers employed and period of service
None
- xiii) Publications/Communications arising from the project during the reporting period
1. Role of Poly (Ethylenedioxythiophene)/Poly (Styrene Sulphonate) on the Performance of Nanocrystalline Titanium Dioxide/Poly (3-Hexylthiophene) Polymer Solar Cells
S Sarathchandran, K Prashanthan, P Ravirajan
Journal of Nanoelectronics and Optoelectronics 6 (3), 272-276
 2. Effect of Temperature and Light Intensity on the Performance of Polymer/Fullerene Solar Cells with Titanium Dioxide Nanolayers
S.Sarathchandran, K.Haridas, Y. Kim, P.Ravirajan,
J. Nanoelectronics and Optoelectronics 5 (2010) 243
 3. Novel Cyclometallated Ruthenium dye sensitizer for nanocrystalline TiO₂ based Solar cells, M.Senthilnathanan, S.Sarathchandran, John.M.Brown, S.Sivaraya and P.Ravirajan, Proceedings of the International conference on "Advances in Continuum mechanics, Nanoscience and Nanotechnology, University of Peradeniya, Sri Lanka, September 26-27, 2008, 240-245.
 4. B. Kajitha, S. Sarathchandran, M. Senthilnathanan and P. Ravirajan, Visible Light Responsive Nanocrystalline Titanium Dioxide for Dye Sensitized Solar Cells, Proceeding of the International Conference on Solar energy Materials, Solar cells and Solar energy Applications (SOLAR ASIA – 2011), 253 (2011).
 5. K. Balashangar, T. Jaseetharan, S. Sarathchandran and P. Ravirajan, Enhancing the Performance of Hybrid TiO₂-Polymer Multilayer Solar Cells by Modifying the TiO₂-Polymer Interface By Single Wall Carbon Nanotube, SOLAR ASIA – 2011, Proceeding of International Conference on Solar energy Materials, Solar cells and Solar energy Applications (SOLAR ASIA – 2011), 258 (2011)

Section 2

Executive Summary of the Project

Seeking a cost efficient alternative to the present day solar cells has received great attention in the last two decades and the solar cells made from organic materials received significant attention.

This project focuses nanostructured polymer based solar cells comprising fullerene electron acceptors. The titanium dioxide incorporated polymer solar cells were also added as one of the major component of this study as TiO_2 could offer several merits. Solar cells were made with a visible light responsive TiO_2 (VLR TiO_2) was also studied in this respect. One of the objectives of this study is that modifying the interfaces within the active layer as well as top electrode in view of enhancing the performance. To acquire better insight in this interface modification, dye sensitised solar cells were made employing both natural and synthesized sensitizers.

The power conversion efficiency (PCE) of polymer / fullerene solar cells having with or without TiO_2 , both having PEDOT:PSS slightly influenced by the temperature and illumination intensity. However the cells with TiO_2 removes the need for PEDOT:PSS which tends to degrade the cell while causing significant increase in the PCE within a 30°C temperature increase speculated to arise from the positive temperature dependence of open-circuit voltage that may be due to a “kink” in the current-voltage characteristics near open-circuit voltage.

In hybrid TiO_2 /poly(3-Hexyl thiophene) (P3HT) solar cells the dependence of polymer uptake when dipping the electrode in the polymer and the role of poly(styrenesulfonate)-doped poly(3,4-ethylenedioxythiophene) (PEDOT:PSS) buffer layer were studied to enhance the performance. Dichlorobenzene was found to be the best dipping solvent with the optimized dipping parameters of concentration, temperature and the time as 1 mg/ml, 120°C and 2 hr, respectively. In the study with the PEDOT:PSS layer the optimum power conversion efficiency (PCE) was observed with the 50 nm thick PEDOT:PSS layer.

Regarding to the application of TiO_2 in dye sensitized solar cells (DSSC), a modified Visible Light Responsive (VLR) TiO_2 has been introduced and found to be promising n-type semiconductor for the DSSC due to the improved optical absorption, dye adsorption and charge transport probably attributed to the high anatase content. In addition to this, both regular and VLR TiO_2 were incorporated with the grape fruit dye and a Ru based synthesized exhibited promising performance which is comparable to solar cells employing commercial dye.

Section 3

Report in detail

I. Introduction and background

The world has to face major challenges in the future because of the rapidly increasing energy demands which cannot be coped with the energy from fossil fuels such as oil and coal which has been formed from the organic remains of prehistoric plants and animals. The extent of fossil fuel on earth is finite so are referred to as non renewable energy sources and their usage should begin to decline after achieving its optimum. Experts predict that the decline in fossil energy production will begin within a decade and play out over a period of about fifty years.¹ According to the reports of International Energy Agency (IEA) the annual Energy consumption had almost doubled during the period starting from 1980 to 2010.² It is also pointed out that over 70% of the increased oil demand is attributable to developing countries. The IEA warned that if this trend in oil demand would continue to persist then it would eventually leads to the global threat of unsustainable path of energy consumption.² In addition to this threat of diminishing in extent the use of fossil fuel causes emission of carbon dioxide to the environment that leads to the environmental pollution and global warming as an unavoidable side effect. According to a report of Energy Information Administration (EIA) more than 75% of the annual Global Carbon dioxide emission is caused by the traditional energy sources.³ The world is thus facing twin energy-related threats: not having adequate and secure supplies of energy at affordable prices and that related to environmental pollution. Therefore alternative renewable energy sources such as wind, hydroelectric, biomass, nuclear, solar thermal and solar photovoltaic are in increasing demand. Among these alternative energy sources the solar photovoltaic energy receives great interest in the recent years compared to others. Moreover the sun is the primary source of energy for all other alternative energy sources. In solar photovoltaic the energy from the sun is directly converted to useful electrical energy. Many countries harness solar energy as a viable option for their electricity needs. In particular, the solar energy will be most useful for tropical countries like Sri Lanka. This source for electricity is particularly preferable if the power consumer station is far remote from the power delivering station. Solar cells that convert solar photovoltaic energy into electricity do not require maintenance once they have been erected and are silent in operation. Above all the earth receives copious amount of solar energy of which an insignificant percentage as small as 1 in 14000 is enough to cater the world wide electricity needs.⁴

Solar cells are characterized by the efficiency with which they can convert incident solar power to useful electric power. Devices utilizing crystalline or amorphous silicon dominate commercial applications which have a record of power conversion efficiency around 20-25 %.⁶ However, efficient crystalline based solar cells, especially of large surface area, are difficult and expensive to produce due to the problems associated with the production of large crystals without significant efficiency-degrading defects while high efficiency amorphous silicon solar cells still suffer from problems with stability. Manufacturing process involves very high temperature and high vacuum. These sufferings felt by silicon devices urges new materials with new fabrication routes. Thus seeking for a cost efficient renewable energy sources has become one of science's major preoccupations and a revolution

has occurred after the introduction of organic solar cells utilizing organic materials, such as conjugated polymers.

Solar cells based on thin organic films are particularly attractive because of their ease of processing, mechanical flexibility, and potential for low cost fabrication of large areas. More over their material properties can be tailored by modifying their chemical properties. The high absorption coefficients exceeding 10^5 cm^{-1} is an asset to these organic solar cells that allow to employ the thin film technology. Although significant progress has been made, the efficiency of converting solar energy into electrical power obtained with thin film organic solar cells still does not warrant commercialization: the most efficient devices have an efficiency around 5%.⁷ To improve the efficiency of these organic solar cells it is crucial to understand the factors limiting their performance. This should target improving the harvest of sunlight, charge carrier generation, transport and collection.

This project focuses nanostructured polymer based solar cells comprising fullerene acceptors. Poly(3-hexylthiophene) (P3HT) polymer and soluble fullerene derivative ([6,6]-phenyl-C₆₁-butyric acid methyl ester) (PCBM) which offered a reproducible efficiencies higher than 4%⁸⁻¹² in several studies have been used in this project. In addition to this, considering the chemical as well as mechanical instability of the fullerene materials, high highlighted attention have been paid to incorporate inorganic stable metal oxides like titanium dioxide with this combination. Furthermore significant time has been spent with solar cells fabricated with nanostructured polymer combined with TiO₂ electron acceptor adopting hybrid structure. The selection of TiO₂ as an n-type material is appropriate for several reasons such as good electron transport properties, stability, ease of fabrication, low – cost and non toxicity and provide opportunity to control the morphology.¹³⁻¹⁸

Modifying the interfaces has been known to enhance the performance. Bearing this in mind the possibility of modifying the interfaces within the active layer with natural and synthesized sensitizers has become a part of this project. Dye sensitized type solar cells were thus fabricated with these sensitizers. Solar cells were made with visible light responsive TiO₂(VLR TiO₂) obtained from the Department of Chemistry, University Of Jaffna, that may possess enhanced absorption and transport properties was also studied in this respect. In the hybrid solar cells the interface within the active layer is a measure of the polymer uptake by the TiO₂ pores. Not only bound to the active layer the study further extended to the interfacial layer below the top electrode with an expectation of enhancing the charge transport.

II. Scientific scope of the project

The ultimate goal of this project is to fabricate solar cells that allow employing the thin film technology. The current efficiency obtained with thin film organic solar cells still does not warrant commercialization: the most efficient devices have an efficiency around 5%. To improve the efficiency of these organic solar cells it is crucial to understand the factors limiting their performance. This should target improving the harvest of sunlight, charge carrier generation, transport and collection.

III. Materials and methods

1. Materials

Poly (3-hexylthiophene) (P3HT) and soluble fullerene derivative ([6,6]-phenyl-C₆₁-butyric acid methyl ester) (PCBM) (styrenesulfonate)-doped poly(ethylenedioxythiophene) (PEDOT:PSS) and TiO₂ are the main materials used in this project.

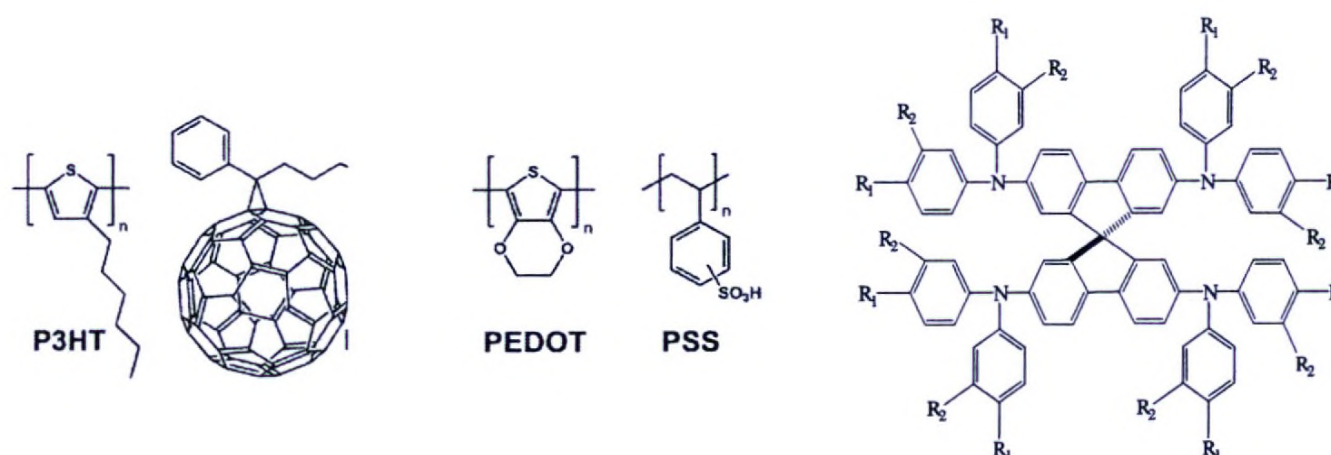


Fig. 1.0: P3HT , PCBM poly(ethylenedioxythiophene)(PEDOT), poly (styrenesulfonate)(PSS) and the Spiro-MeOTAD solid state hole transporting material

The solid state hole transporting material Spiro-MeOTAD supports to mitigate the adverse effects caused by a liquid hole transporting material in a dye sensitized solar cell.

Natural, commercial and synthesized sensitizer prepared by Dr. M.Senthilnathanan, Department of Chemistry, University of Jaffna are some other materials employed in this project .

2. Experimental techniques

UV-VIS. optical absorption spectroscopy, Fourier Transform Infra Red Spectroscopy (FTIR), transient absorption spectroscopy (TAS), photoluminescence quenching, general fabrication technique, four probe and Van der Pauw technique have been employed in this project.

2.1 Fabrication and characterisation of P3HT:PCBM solar cells

Indium-tin oxide (ITO)-coated glass substrates ($\sim 25\Omega/\text{cm}^2$) were first cleaned several times thoroughly in acetone and isopropanol and then annealed to remove any organic residue. They were then blown with nitrogen gas. To prepare the dense TiO₂ nanolayer, precursor solution was prepared using titanium isopropoxide and acetylacetone as described in the Ref. [19] for the hole blocking purpose. A dense layer of TiO₂ was made on the ITO glass using the spray pyrolysis technique and sintered at 450 °C for 30 minutes. Blend solutions were prepared with P3HT and PCBM, purchased from Merck Chemicals Ltd, with a 1:1 weight ratio in chlorobenzene at a solution concentration of 25 mg/ml. These solutions were vigorously stirred for more than 24 hours to maximize mixing. The blend solution of P3HT:PCBM was then spin-coated onto this substrate (1250 rpm) after which the films were annealed at 120 °C for 120 minutes in an N₂ environment. Some of the

devices were with PEDOT: PSS layer onto this substrate. To make the PEDOT:PSS layer, the aqueous solution of PEDOT:PSS (Baytron) after filtering through a 0.45 μm filter was heated at 90 $^{\circ}\text{C}$ for 5 minutes.²⁰ It was then spin-coated at 4000 rpm. The substrates were again baked at 100 $^{\circ}\text{C}$ for another 5 minutes in the nitrogen environment. Finally, gold top contact was made by thermal evaporation at a pressure better than 5×10^{-6} Torr. After that they were annealed at 120 $^{\circ}\text{C}$ for 10 minutes in a home-built annealing box filled with nitrogen. The current-voltage (I-V) measurements (using a Keithley 2400 source meter) of these photovoltaic devices were carried out in a closed cycled cryostat using He gas and in a furnace both in the dark and illumination under white light.

2.2 Fabrication and characterisation of nanocrystalline TiO_2 /polymer solar cells

TiO_2 paste (purchased from Dysol) was dissolved in Tetrahydrofuran (110 mg ml^{-1}) and the TiO_2 solution was spun cast onto the cleaned glass plate and sintered at 450 $^{\circ}\text{C}$ for 30 min. The polymer solution in which the TiO_2 coated glass plates were dipped was prepared in six different solvents and the optical absorption was taken for these electrodes, The P3HT solution concentrations, dipping time, dipping temperature were the parameters studied.

Indium-tin oxide coated glass substrates (25 Ω/cm^2) were cleaned adopting the usual procedure as described for the glass substrates. The precursor solution to deposit the dense TiO_2 nanolayer, prepared as described in the Ref. [8], was sprayed onto the ITO substrates and subsequently sintered at 450 $^{\circ}\text{C}$ for 30 minutes. This dense TiO_2 layer avoids a direct contact between poly(3-Hexylthiophene)(P3HT) and ITO substrate which would short circuit the device. The porous nanocrystalline TiO_2 film was deposited on the dense TiO_2 . After allowing sufficient time for the substrates to cool down they were then dipped in the P3HT (purchased from Merck Chemicals Ltd) solution possessing the optimum dipping conditions. After blown with nitrogen gas they were soft baked at 50 $^{\circ}\text{C}$ for 5 min and P3HT layer (~50 nm thick) was spun on this substrate.

Filtered PEDOT: PSS (BAYTRON) layer was then spin-coated at a spin rate of 4000 rpm onto the P3HT layer. The samples were again baked at 100 $^{\circ}\text{C}$ for 5 min in a nitrogen filled home-built annealing box. Devices were made by the deposition of silver film on the PEDOT:PSS layer under vacuum below 10^{-5} Torr in the chamber of the thermal evaporator. A dot of silver paint was applied on top of this silver film and on the ITO bottom electrode for better contact and subsequently annealed at 120 $^{\circ}\text{C}$ in the nitrogen environment.

In order to further enhance the performance the solar cells were made with the PEDOT:PSS layer with varying thickness. Filtered PEDOT: PSS (BAYTRON) solution was spin-coated at different spin rates ranging from 1050 rpm to 10100 rpm onto the P3HT layer. The samples were again baked at 100 $^{\circ}\text{C}$ for 5 min in a nitrogen filled home-built annealing box. Solar cells were made by the deposition of silver film on the PEDOT:PSS layer under vacuum below 10^{-5} Torr in the chamber of the thermal evaporator.

2.3 Modification of interfaces using natural and synthesised sensitizers

2.3.1 Preparation of sensitizers

Distilled water was added to scraped beetroot, crushed jambolan white yam tuber and grape fruit coat and the mixtures were shaken at room temperature for one hour. The

solution was filtered and then the solvent was removed completely in a rotatory evaporator. The commercial dye *cis*-bis(isothiocyanato)(2,2'-bipyridyl-4,4'-dicarboxylato)(2,2'-bipyridyl-4,4'-di-nonyl) ruthenium(II), abbreviated as Z907, and novel Ru based sensitizer sensitized by Dr. M. Senthilnathanan, Ru(2-phenyl-4-quinolinecarboxylic acid)bis(2,2'-bipyridine)(PF₆) (MUJA1) were prepared in acetonitrile-*tertiary* butanol (1:1 v/v) with concentration 0.3 mM.

Nanocrystalline TiO₂ films of thickness 4.7 μm / 200 nm were prepared on indium doped tin oxide (ITO) / fluorine doped tin oxide (FTO) glass plates by doctor blading / spin coating method respectively. The films were then sintered at 450°C for an hour. The dyes were coated on the nanocrystalline TiO₂ electrodes by dipping the electrode in the respective dyes for 24 hours. Absorption and photoluminescence (SPEX 750M) measurements of the dye coated TiO₂ films were taken. Spiro-MeOTAD dissolved in toluene was deposited on each dye / TiO₂ electrode using spin coater. PEDOT spin coated FTO glass/ Pt coated FTO was used as the counter electrode. The device was simply made by pressing the two electrodes. The current-voltage (I-V) measurement of these solar cells was carried out in the dark and under solar simulator of intensity 100 mWcm⁻² using Keithley-2400.

2.3.2 Fabrication of solar cells and characterization

Absorption measurements of each dye solution, and dye coated TiO₂ electrodes were carried out. FTIR spectroscopy of each dye coated TiO₂ electrode was obtained by using FTIR spectrometer. Dye sensitized solar cells were fabricated with each sensitizer as described in the following lines.

The current- voltage measurement of each dye sensitized solar cell was done in dark and under solar simulator with AM 1.5 spectral filter using a computer controlled Source Measure Unit (Keithley-2400). External quantum efficiency measurements were done using calibrated photo diode (Newport) and computer controlled SPEX-750M spectrometer. In this measurement, the wavelength of the incident light was changed from 400 nm to 700 nm and corresponding photocurrent of the solar cells was observed.

IV. Results/outputs and Discussion

1. Enhanced performance shown by inverted solar cells

Figure 1 shows that the current density–voltage (J-V) characteristics of an inverted device without PEDOT:PSS (ITO / dense TiO₂ / PCBM:P3HT /Au) in a temperature range varying from 30 °C to 75 °C prominently differ from the other solar cells in that a 'kink' exhibited in the vicinity of the open-circuit voltage, V_{OC}. In this vicinity, the slope of the J-V curve for voltages less than V_{OC} (V_{OC} -ΔV, infinitesimal ΔV is assumed to be positive) is very sensitive to both the temperature and intensity, compared to for voltages greater than V_{OC}. It should be noted that the inverse of the slope represents series resistance and it follows that the series resistance shifted to a higher value when the applied voltage passed the V_{OC} from V_{OC} -ΔV to V_{OC} +ΔV. Although the kink had been observed in some other previous studies²¹⁻²³, the power conversion efficiency, controlled to a considerable extent by the kink, is the main outcome that distinguishes this study from those observations and studies. Moreover, this kink effect becomes dominant with an increase in temperature or intensity.

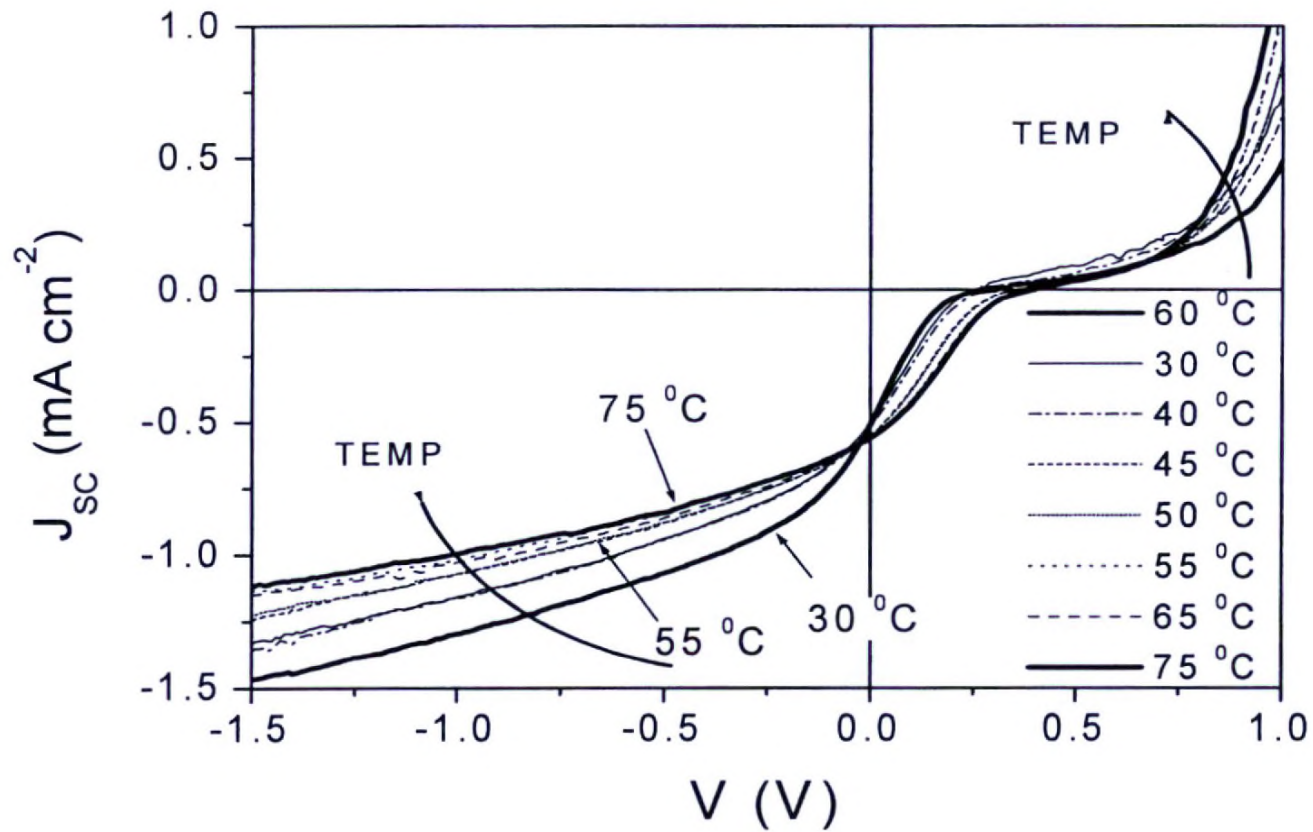


Fig.2: Current-voltage characteristics of ITO / dense TiO₂ / PCBM: P3HT / Au device at different temperatures and under white light illumination of intensity of 10 mW cm⁻².

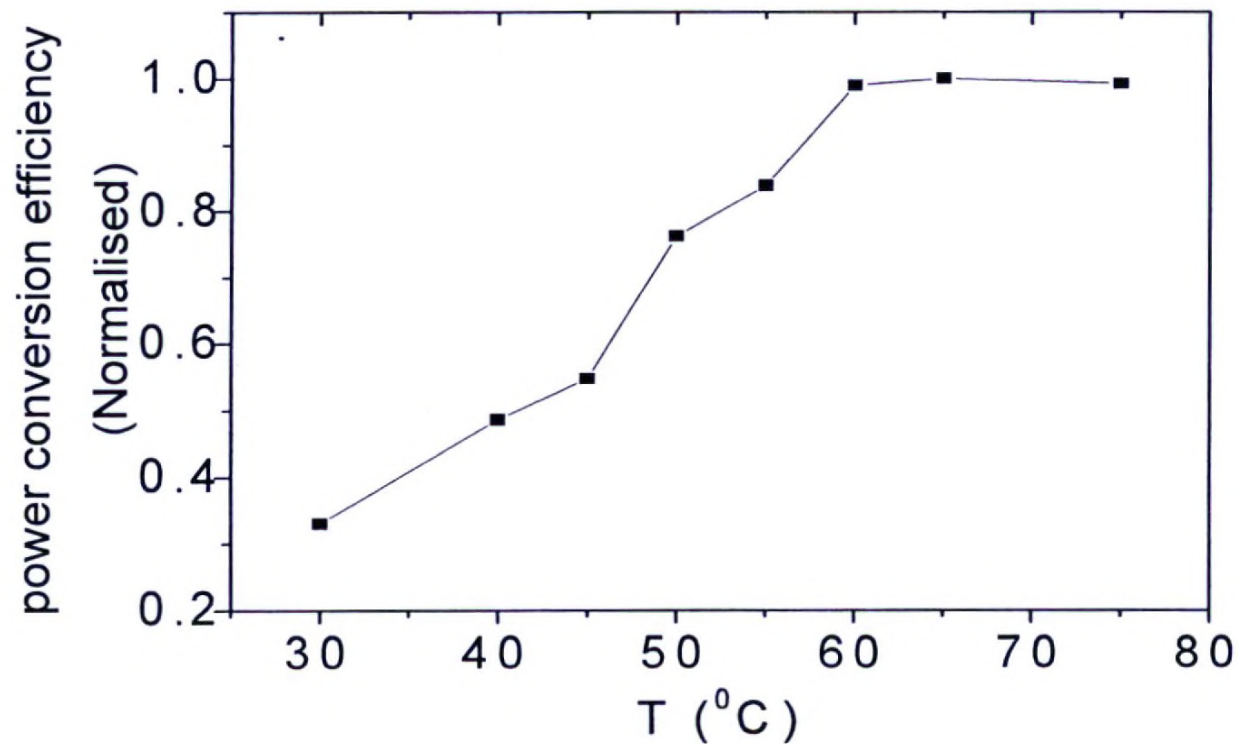


Fig.3: Normalized power conversion efficiency of ITO / HBL / PCBM:P3HT / Au at different temperatures

Figure 3 shows that the power conversion efficiency of the inverted PCBM:P3HT solar cells with a TiO₂ nanolayer significantly increases (nearly a factor of 3) with temperatures in the range of 30 °C to 65 °C. The strongly temperature-dependent open-circuit voltage with a positive temperature coefficient in the temperature range of 30 °C - 65 °C is the major underlying reason for this strange behavior in terms of the power conversion efficiency. The very similar trends of temperature responses in relation to power conversion efficiency and the open-circuit voltage (as depicted in

Fig.4 and Fig.5) further support that the power conversion efficiency mostly relies on the open-circuit voltage.

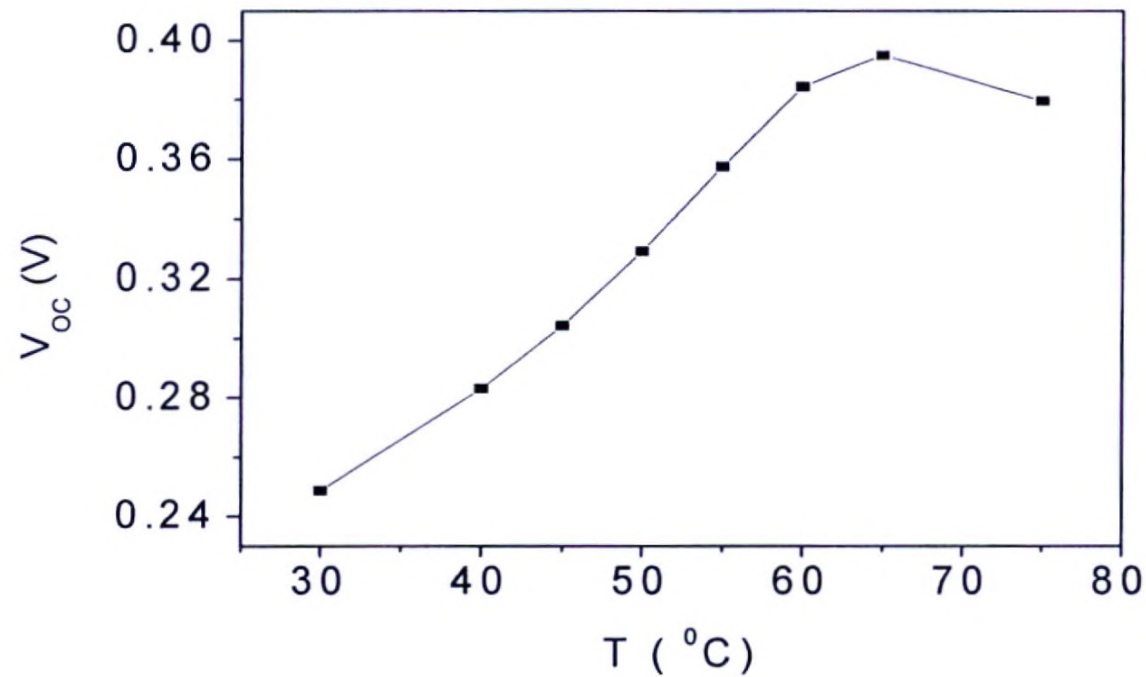


Fig.4: Open-circuit voltage of the inverted solar cell, ITO / dense TiO₂ / PCBM: P3HT / Au.

For a solar cell that behaves as a non-ideal diode, current density J is given approximately by

$$J = J_{SC} - J_0 [\exp(eV / mkT) - 1] \quad (1)$$

Where J_0 is the dark saturation current density, m is the ideality factor, k is Boltzmann's constant and T the temperature.²⁴ Open-circuit voltage, V_{OC} , is then related to short-circuit current, J_{SC} through

$$V_{OC} = \frac{mkT}{e} \ln \left[\frac{J_{SC}}{J_0} \right] \quad (2)$$

Substituting for J_0 one could obtain the expression²³

$$V_{OC} = a - bT \quad (3)$$

Where a and b are constants involving the intrinsic parameters of the active material. The linear decrease of V_{OC} with temperature as governed by equation (3) was observed in several structures. A linear decrease of V_{OC} with average temperature coefficient $\frac{dV_{OC}}{dT} = -(1.40 - 1.65) \text{ mV}/^\circ\text{C}$ has been reported for typical PCBM/P3HT cells with PEDOT:PSS buffer layer within a temperature range of 30 °C to 60 °C.²⁵ However, V_{OC} of the inverted solar cell shows almost linear increase with temperature, having an average temperature coefficient of $\frac{dV_{OC}}{dT} = +6.9 \text{ mV}/^\circ\text{C}$

violating the non-ideal diode model.

At V_{OC} dark current is compensated by the current under illumination and hence making the zero photocurrent. If the kink effect was not present, there would be no discontinuity of the slopes of J-V curve at the V_{OC} which leads to the decrease in V_{OC} similar to the conventional devices, which is not the real case. This supports the kink-controlled V_{OC} .

It has been reported in the literature about the strong temperature dependence of J_{SC} of the polymer: fullerene solar cells.²⁵⁻²⁷ In our case, J_{SC} exhibits an increasing trend on temperature, attains the maximum around 65 °C and falls down with the further increase in temperature. The fill factor of the polymer: fullerene solar cells is usually

low compared to the other structures because of the possible shunt pathways present due the blend nature. In the inverted solar cells, the FF becomes even lower because of the kink.

Figure 4 shows the current density-voltage characteristics of the inverted solar cell at a temperature of 65 °C under different low light intensities. In this intensity range, the scaling exponent is found to be unity which shows that the dominant mechanism for recombination is monomolecular type. A significant deviation from unity for the value for the scaling exponent could be expected when the mode of recombination changes from monomolecular to bimolecular recombination, particularly at higher light intensities. As a consequence of the linear variation of J_{SC} with P_{in} , it follows from equation (2) that V_{oc} should exhibit a slope of mkT/q , when plotted as a function of the logarithm of light intensity. The ideality factor of the inverted devices is found between 1.5 and 2.0. This kink effect becomes dominant at higher temperature and/or intensity. In order to explore the origin of this kink, we examined the J-V characteristic of the device by varying the light intensity and wavelengths. The kink feature persists at different wavelengths, indicating that the kink is not a result of the spatial distribution of the photogeneration rate, and under different light intensity, indicating that it is not due to charge trapping. The kink may however be due to the energy barrier at TiO_2 / fullerene or P3HT/Au interface.

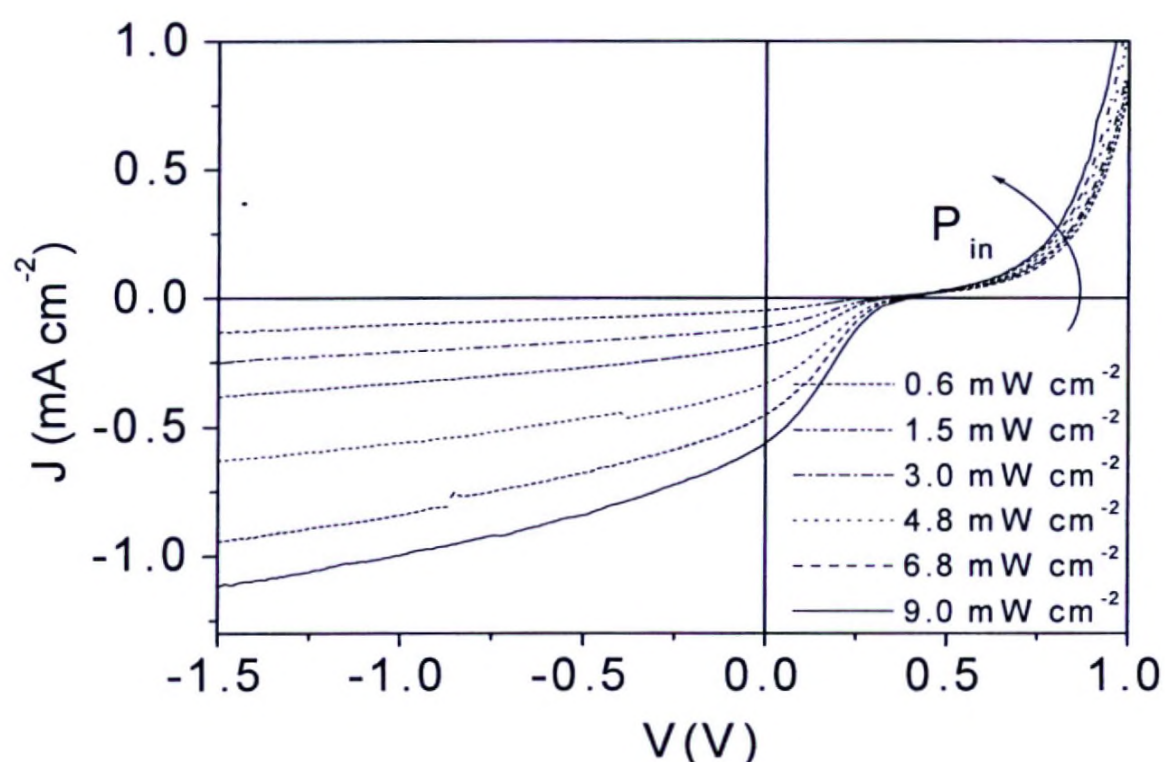


Fig. 5: Current density-voltage characteristics of ITO / HBL / PCBM: P3HT / Au at a temperature of 65 °C under different white light intensities ranging from 0.6 mW cm⁻² to 9 mW cm⁻².

2. Enhancing the performance of TiO_2 /polymer solar cells

2.1. Identifying optimum dipping solvent parameters

The dependence of the best dipping parameters: solvent to prepare P3HT solution, concentration of the solution, dipping temperature and dipping time have been systematically studied. based on the optical absorption studies. The optimised

dipping parameters were found to be 1 mg/ml concentration, 2 h dipping time, 110 °C dipping temperature with dichlorobenzene solvent.

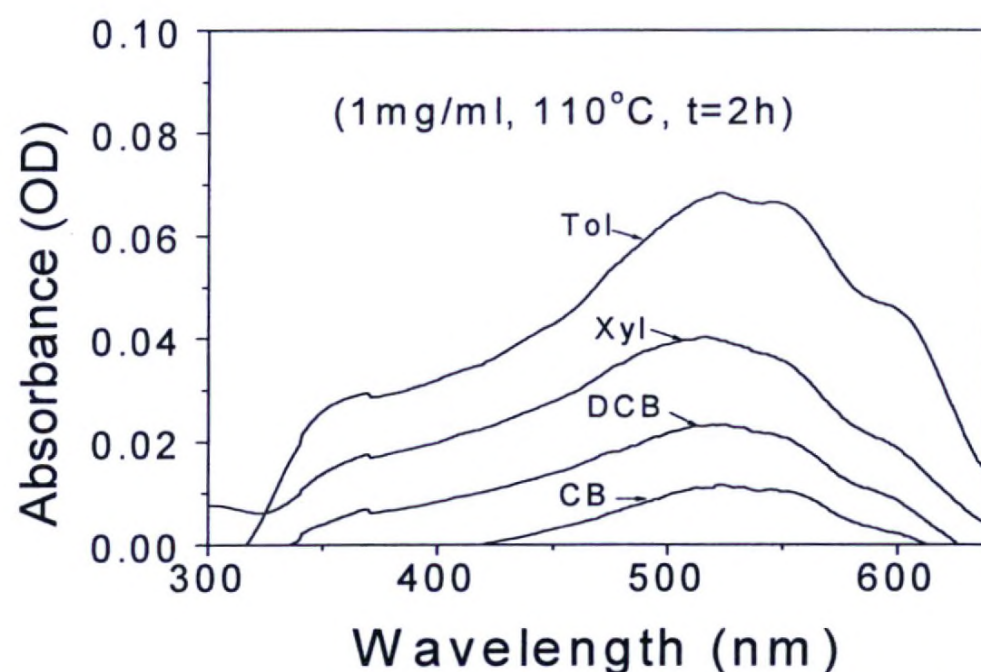


Fig 6: Optimized optical Absorption at $[T] = 110\text{ }^{\circ}\text{C}$, $[c] = 1\text{ mg/ml}$ at a particular dipping time $t = 2\text{ h}$ with Chlorobenzene (CB), Dichlorobenzene (DCB) and Xylene (Xyl) and Toluene (Tol)

The current density (J)–Voltage (V) characteristics of the hybrid TiO_2 /P3HT multilayer devices with different PEDOT:PSS thickness characterized both in dark and under the AM 1.5 illumination from a solar simulator with an intensity of 70 mW/cm^2 is shown in the Fig. 5.2.

The forward biased dark current, observed to increase in the previous studies with hybrid nanostructured TiO_2 /polymer multilayer devices upon inclusion of the PEDOT:PSS under layer,^{17,28} almost showed the same increasing trend with the present case with increasing PEDOT:PSS thickness. However the dark current rectification ratio was observed to decrease when the thickness of the PEDOT: PSS layer was continuously increased up to about 80 nm and again increased when the thickness exceeded 90 nm. But the PEDOT: PSS layer that exceeded 100 nm thickness suffered peeling off from the substrate and for this reason this analysis was limited with those having not too thick PEDOT: PSS layers although techniques like encapsulation might, however, find remedy for this problem identified with thick PEDOT: PSS layers. The previous reports account the reduction of polymer/metal electrode energy barrier for the injection of holes for the drop in serial resistance and subsequent increase in dark current, current under illumination and the absence of a distorted feature near the open-circuit voltage as well as the little reduction in the open-circuit voltage resulted by the inclusion of PEDOT: PSS layer.³⁰

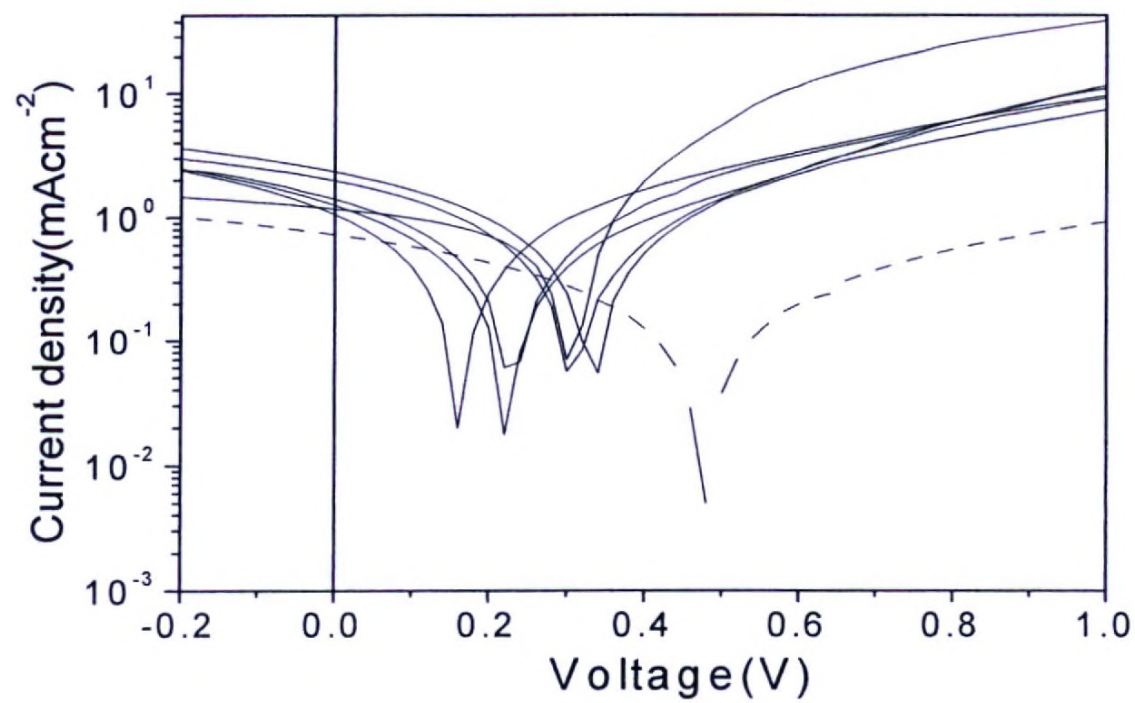
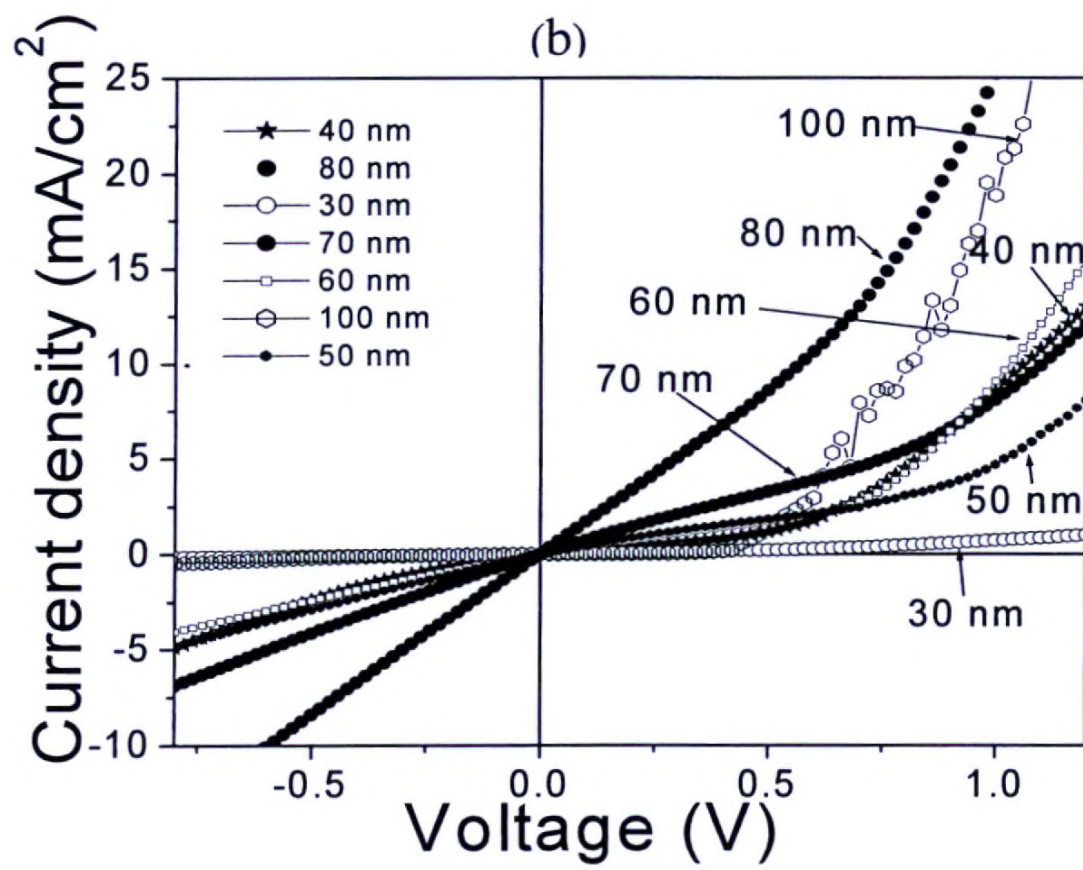
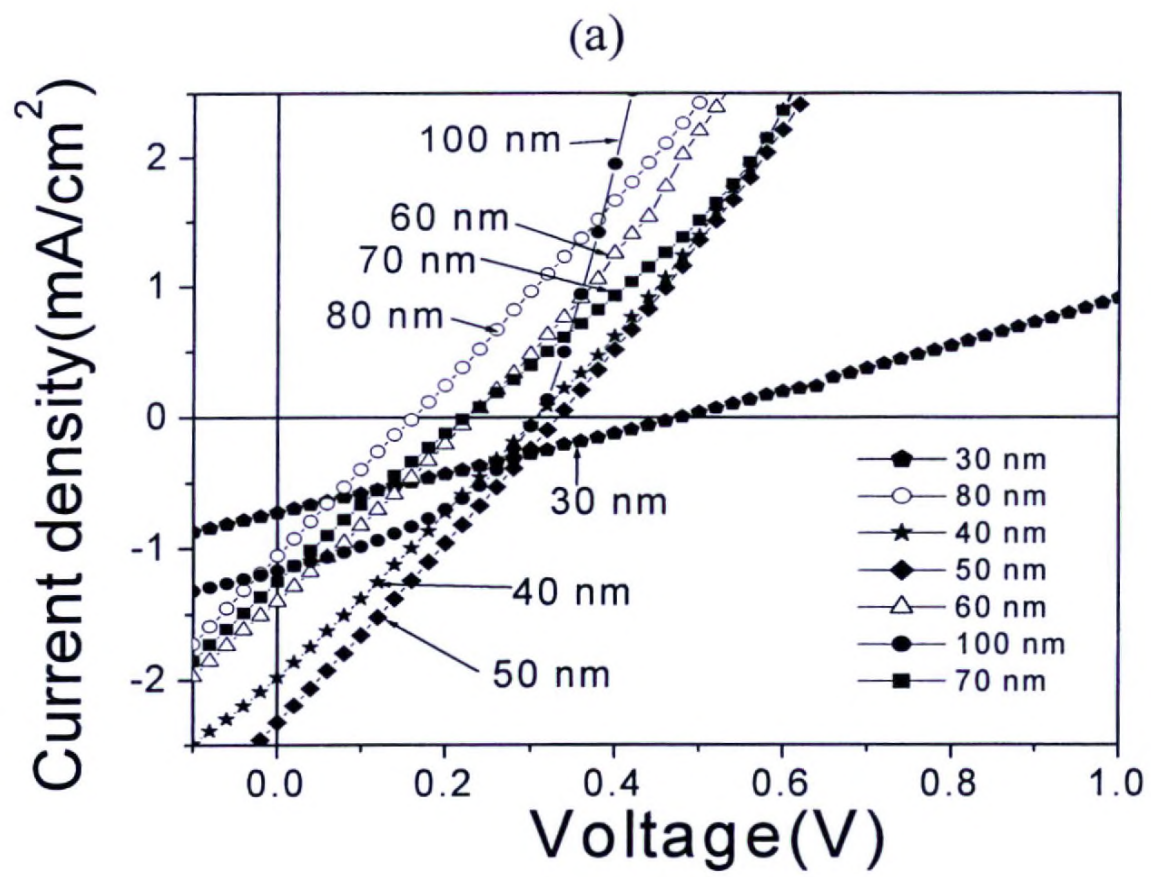


Fig. 7: Current density (J)–Voltage (V) characteristics of the hybrid TiO₂ /P3HT multilayer devices with different PEDOT thickness (a) in dark and (b) under AM 1.5 illumination from a solar simulator with an intensity of 70 mW/cm² (c) Replotted light J-V characteristics for better observation of the change in open-circuit voltage

In this study, the open-circuit voltage (V_{OC}) started to fall continuously, reaching the minimum and seems to increase again for the devices with reasonably thick PEDOT:PSS layers (≈ 100 nm) as could be seen in the Fig.2. The short-circuit current density (J_{SC}) is maximized with the thickness of the PEDOT:PSS layer around 50 nm. A rather low value, around 0.3 was yielded for fill factor (FF) even when the illumination intensity reached a value as high as 100 mW/cm². Another significant observation is the reasonably improved FF yielded for the device with 100 nm thick PEDOT:PSS further strengthening the improved dark rectification. However the optimum power conversion efficiency was observed with about 50 nm thick PEDOT:PSS layer as shown in the Fig. 2. We should note that power conversion efficiency was optimized not in absolute terms but only entailed the relative variation with the PEDOT:PSS thickness since some of the steps like the dye dipping prior to the dipping in the polymer solution have been skipped in this study for simplicity. Similarly the identical steps followed in the preparation of the dense TiO₂ hole blocking layer which is known as vital for the optimization of the performance removes the influence of the quality of the dense TiO₂ hole blocking layer on this comparative study.

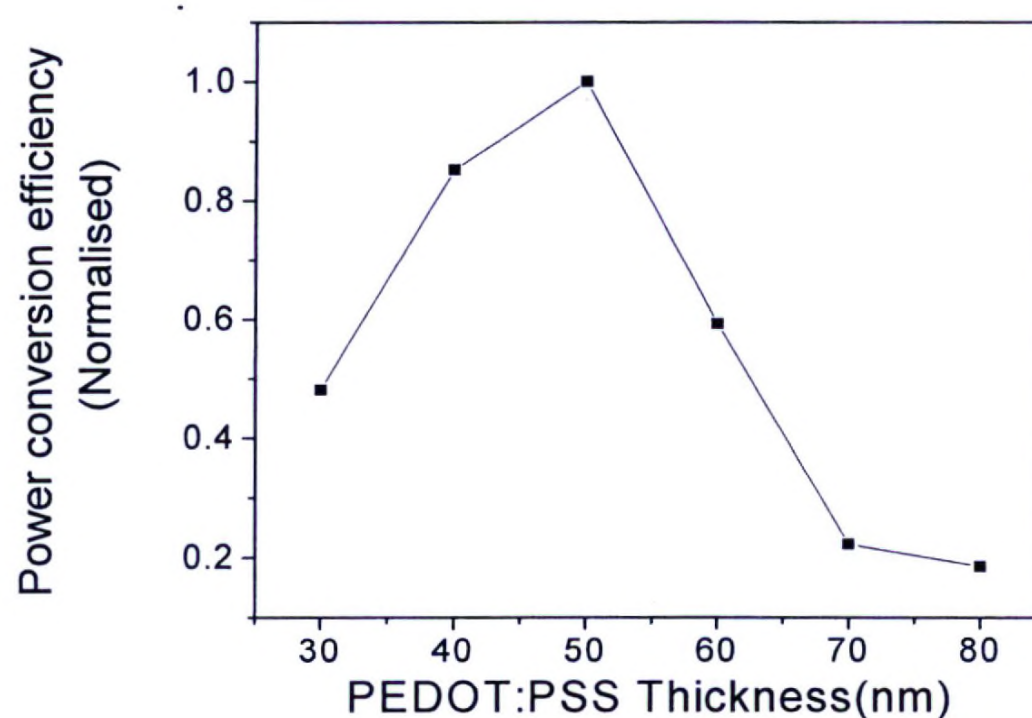


Fig. 8: Normalized Power conversion efficiency of the hybrid TiO₂ /P3HT multilayer devices with different PEDOT: PSS thickness (30, 40, 50, 60, 70, 80 nm) under the stimulated illumination with 70 mW/cm² light intensity.

The relatively higher J_{SC} and moderate value of the V_{OC} among the others responsible for the optimized power conversion efficiency depicted by the devices with PEDOT:PSS layer thickness around 50 nm. Comparatively inferior power conversion efficiencies shown by the devices with 70 nm and the 80 nm thick PEDOT:PSS layers mainly resulted from poor V_{OC} .

A number of factors associated with the PEDOT:PSS layer such as morphology related compactness and uniformity, well-adherence to the surface of P3HT and their

possible influences on polymer/metal energy barrier, series and shunt resistance, mode of recombination and the diffusion of the silver nanoparticles collectively responsible for the observed behaviour and thereby have control on the photovoltaic parameters J_{SC} , V_{OC} and FF. The reduction of the energy barrier already confirmed in the previous studies^{17,18} could be connected with the particle arrangement in the PEDOT:PSS layer as better compatibility or match with the polymer layer, reduction of the surface roughness and the filling of voids contributes in the reduction of the series resistance²⁹ that enhances the collection of charges that leads to reduce the series resistance. In the too thin layers it cannot be expected the better compatibility. It is reasonable to assume a saturated level for the enhancement in the charge collection due to the morphology and the reduction in series resistance as well when the thickness increased up to a certain extent beyond which the series resistance tends to increase mainly receiving contributions from layer resistance itself. The inverse of the slope of J-V curve near V_{OC} in Fig.2 (a) as a measure for series resistance confirms and agrees with the above argument. Furthermore, the layer resistance receives importance due to the hygroscopic nature of the PEDOT:PSS layer that decrease the conductivity. The shunt resistance, on the other hand, is a measure of the inverse of the slope of J-V curve near J_{SC} . Non compact and non uniform films probably lead to pinholes acting as shunt pathways that degrade the performance. The effect of the diffusion of silver nanoparticles towards the P3HT through the PEDOT:PSS is not well understood, but if the diffusion meeting a critical stage then it would be a valid argument that the increased shunt pathways leads to a decreasing effect on the shunt resistance. The shunt resistance in this analysis, showed an initial steep fall followed by gentle decrease and again a steep increase with the PEDOT:PSS thickness reflecting the trend shown by V_{OC} .

The charge carrier recombination is another important aspect remaining for the discussion which usually tends to reduce the photocurrent and/or photo voltage. The recombination generally depends on macroscopic film properties such as the size and shape of the devices and the nano scale phase-separated regions, percolation paths²⁶, molecular arrangement and traps as well. In the devices having too thin or too thick PEDOT:PSS layers, slower rate of charge carrier collection expectable than the rate of generation that in turn leads to the recombination as a dominant process. It is also reasonable to expect recombination even worse in the thin PEDOT:PSS layer devices due to the inefficient electron blocking function carried out by thin PEDOT:PSS layer.

Another important observation is the ageing effect affected the performance in a somewhat unexpected manner, the optimum power conversion efficiency shifted to that corresponds to 80 nm thick PEDOT:PSS layer about 30 weeks of time elapsed after the fabrication. Significantly increased V_{OC} and the more stable J_{SC} are the main causes for the much improved performance of the devices generally having PEDOT:PSS layer thickness above 60 nm. The Fig.4 illustrates the variation of the J_{SC} and V_{OC} of the aged devices with the light intensity.

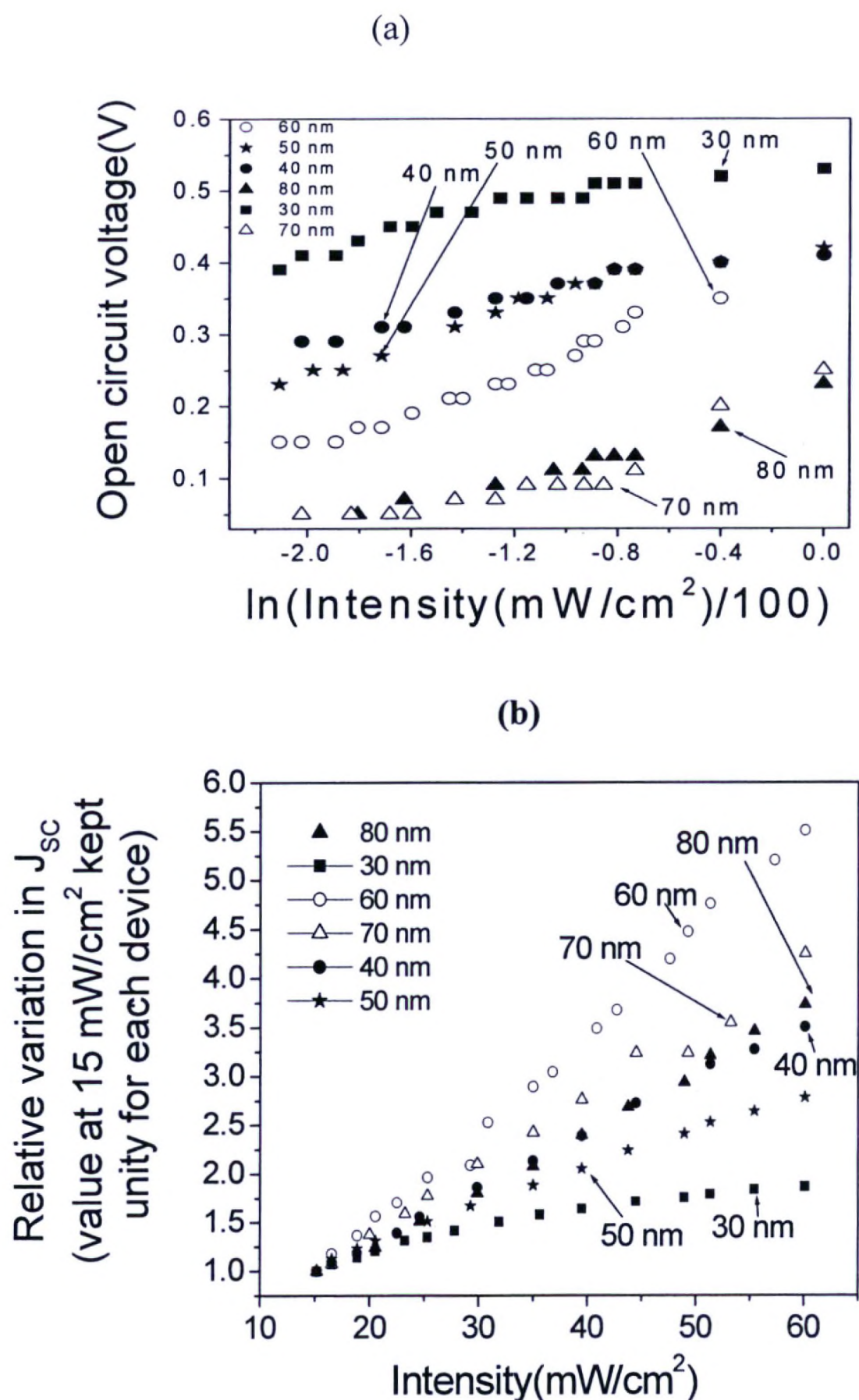


Fig. 9: Variation in the (a) open-circuit voltage with $\ln(\text{intensity})$ and (b) short-circuit current density with the intensity relative to a very low intensity 15 mW/cm^2 of the ITO/dense $\text{TiO}_2/\text{layer}/\text{porous TiO}_2/\text{layer}/\text{P3HT}/\text{PEDOT:PSS}/\text{Ag}$ devices with varying PEDOT:PSS thickness(x nm) after 30 weeks time elapsed (kept under vacuum)

Figure 9 (a) shows the significant increase in the V_{OC} compared to the as prepared devices. The sublinear variation of J_{SC} with the intensity suggested the bimolecular recombination could be assigned to the thin PEDOT:PSS layer devices which was further evidenced by the scaling exponent α found from the graph of $\ln J_{SC}$ Vs $\ln I$ that yield a value close to 0.5 in the power law relationship $J_{SC} \propto I^\alpha$ relating the short-circuit current density J_{SC} and intensity I . A detailed study regarding stability can only handle these observations efficiently. Anyhow the long term stability as well as the more stable J_{SC} and the significant increase in the V_{OC} found in the devices with reasonably thick PEDOT:PSS layers may be a figure of merit most probably attributable to the diffusion of silver nanoparticles.

3. Interface modification using sensitizers

New features seen in the absorption spectrum of dye adsorbed TiO_2 compared to that with bare TiO_2 electrodes is a consequence of adsorption of dye molecules on the TiO_2 surface, known as the dye sensitization. All the four natural sensitizers exhibited broad optical absorption spectra in the visible region. The absorption features were compared with Z907.

Absorption features of natural dyes from white yam tuber, jambolan fruit, beetroot and commercial dye are comparable with a peak around 530 nm. Dye from fruit coat of Grapes shows better absorption peaking at 550 nm (Fig 10 a). The absorption property is strengthened in the dye adsorbed TiO_2 than that of dye alone for the Jambolan fruit dye.

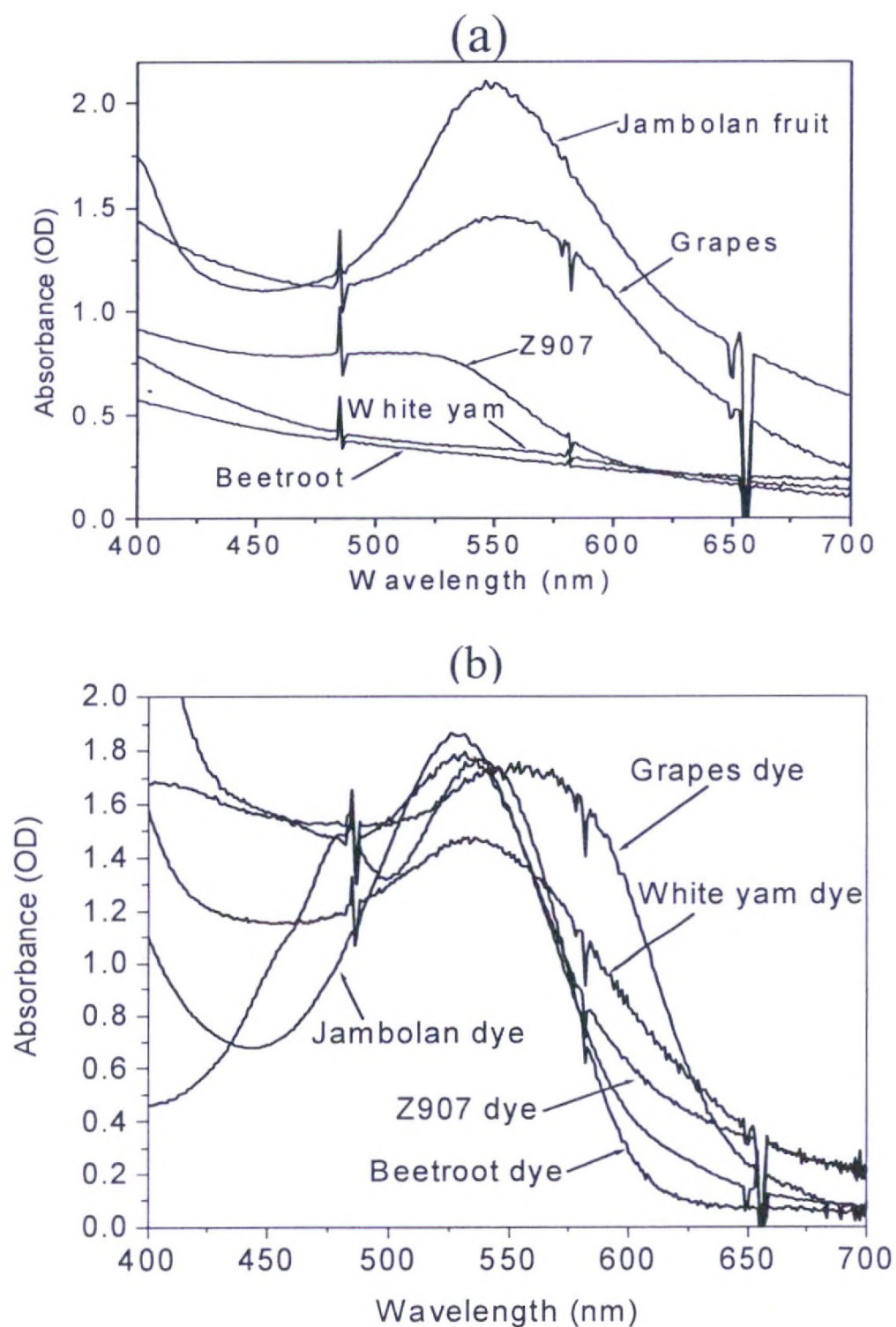


Fig. 10: UV-VIS Spectroscopy of (a) Dye solutions alone (b) Dye adsorbed TiO_2

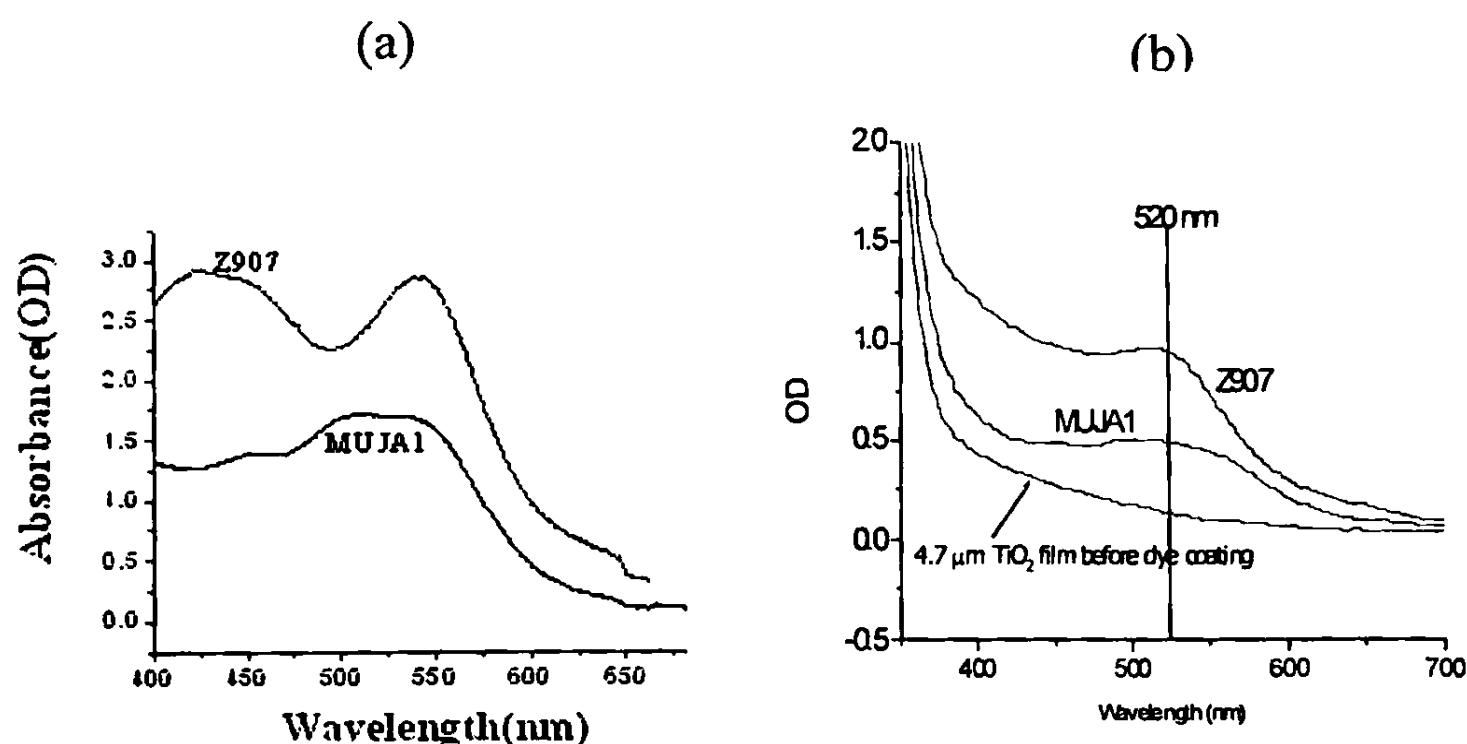


Fig. 11: Optical absorption of (a) MUJA1 and Z907 (0.3 mM solution)

(b) MUJA1 and Z907 dye on 4.7 μm TiO_2 films.

Figure 11(a) shows the absorption spectra of the dye solutions in acetonitrile-*tertiary* butanol (1:1 v/v) solvent while the figure 3(b) shows the absorption features of dye coated TiO_2 films of thickness 4.7 μm . MUJA1 shows a broader absorption peak compared to Z907, which is a striking and encouraging feature. However, the absorbance of MUJA1 is lower than that of Z907, which could be due to smaller extinction coefficient of MUJA1 compared to Z907. The presence of two carboxylic acid groups in Z907 enhanced its adsorption on TiO_2 film. It prompts further modifications in the structure of MUJA1 to improve its attachment to TiO_2 surface and shift its absorption to a longer wavelength.

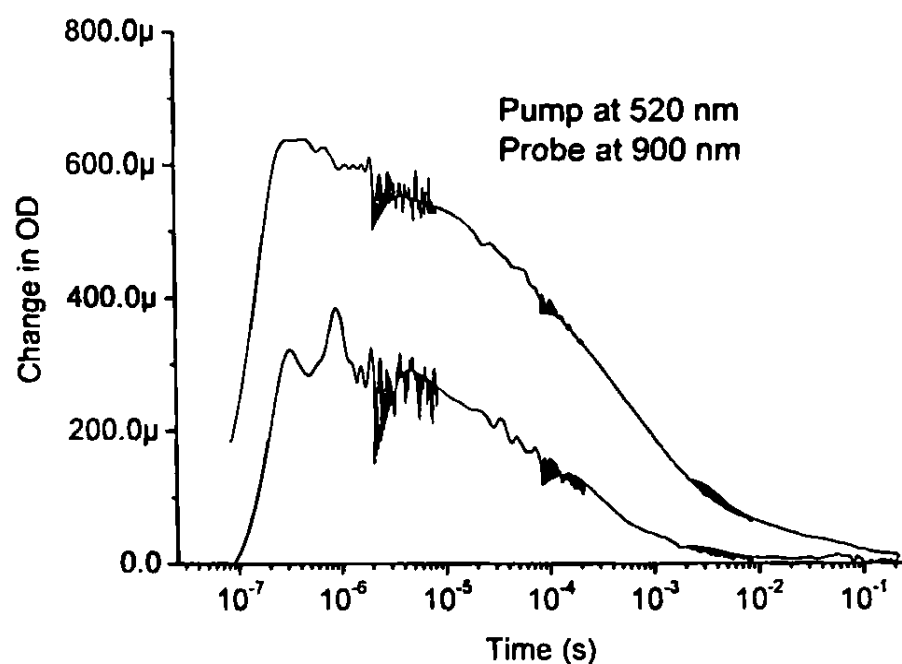


Fig. 12: Transient absorption due to dye cation at 900 nm following laser pulse excitation at 520 nm, at an excitation density of 75 $\mu\text{J}/\text{pulse}/\text{cm}^2$. The decay is assigned to recombination between electrons in TiO_2 and dye cation. This was carried out by Prof. P.Ravirajan at the Imperial College, London.

Figure 12 shows the recombination kinetics of the dye in nanoporous TiO_2 / dye structure. The charge recombination in porous TiO_2 / MUJA1 is slow with a half-life of 100 μs , which is similar to porous TiO_2 / Z907 structure, although charge transfer yield is low due to smaller extinction coefficient.

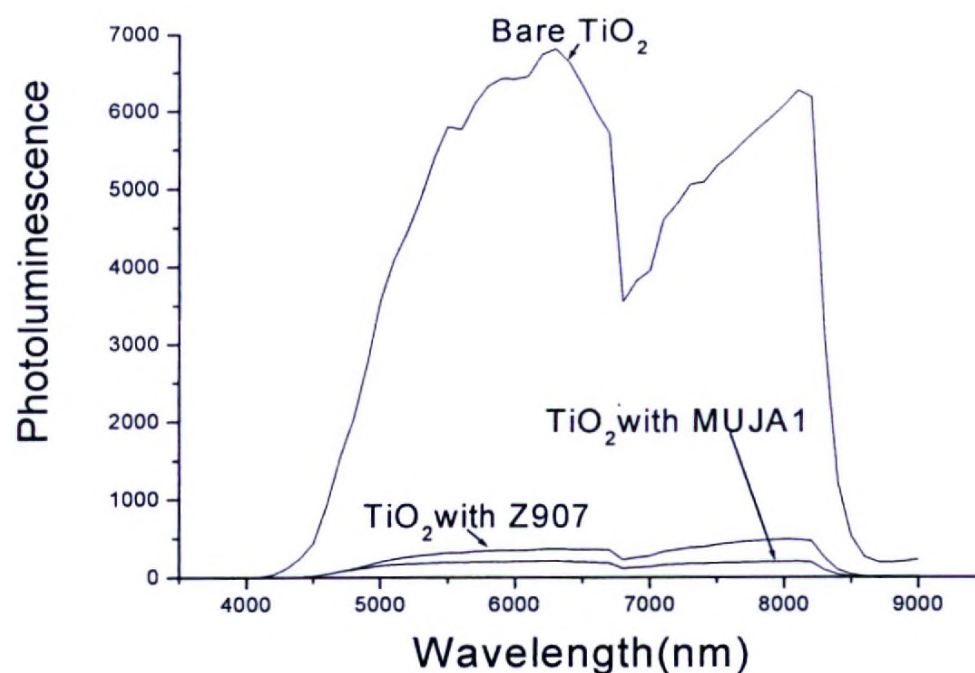


Fig. 13: Photoluminescence spectra obtained for bare TiO_2 and dye adsorbed TiO_2

Intensity of photoluminescence spectrum is a measure of the electron-hole recombination process. Figure 13 shows photoluminescence study of bare TiO_2 and the dye adsorbed TiO_2 . It explicitly depicts that application of both dyes highly quench the photoluminescence intensity. This shows that MUJA1 dye should offer good device performance like Z907. Device fabrication and analysis of its performance are in progress and will be reported in the conference.

The surface area of the TiO_2 nanoparticle is another important aspect to be taken into account as far as the dye adsorption is concerned.

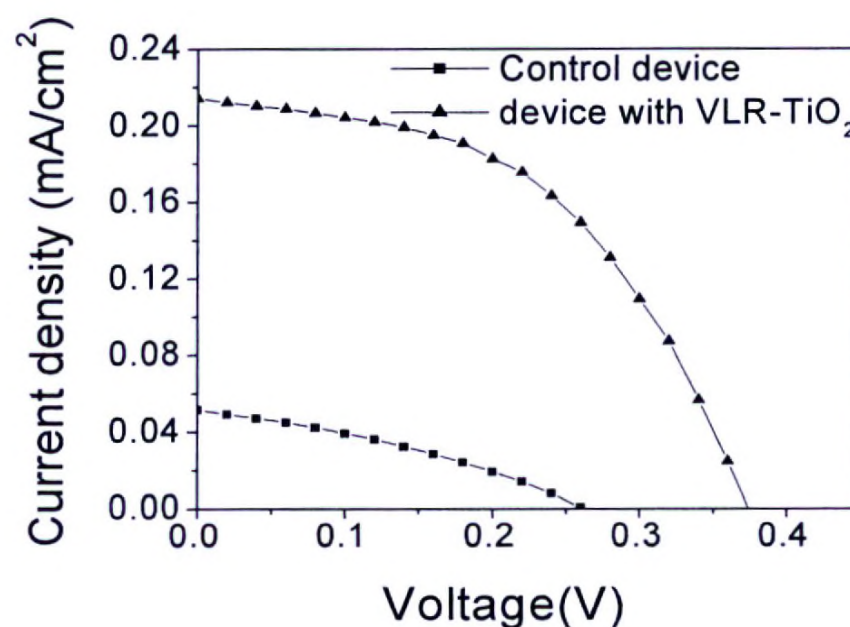


Fig. 14: Comparison of current density-voltage characteristics of solar cells having VLR- TiO_2 and TiO_2 .

The Figure 14 illustrates the current density-voltage characteristics of the solar cells utilizing VLR- TiO_2 and commercial TiO_2 both of these employing grape fruit coat dye. More than a factor of three increase observed in the short-circuit current density whereas the open-circuit voltage shown an increase of about 42 % in the solar cells utilizing VLR- TiO_2 . Highly anatase content in VLR- TiO_2 ^{31,32} could explain for the enhanced photovoltaic performance. It has been reported that the high anatase TiO_2 could facilitate the electron transport.

V. Conclusion

This project covers multidisciplinary themes of the polymer based solar cells giving significant attention to the TiO₂ incorporating solar cells. Main conclusions drawn in this project will be summarized as follows:

1. In the polymer blend solar cells, the power conversion efficiency of both the conventional cells having P3HT:PCBM and the polarity inverted design achieved by the introduction of TiO₂, both having PEDOT: PSS slightly influenced by the temperature and illumination intensity. Power conversion efficiency of the inverted solar cells without PEDOT: PSS is increased over a factor of three within a 30 °C temperature increase speculated to arise from the positive temperature dependence of open-circuit voltage which may be due to a “kink” in the current-voltage characteristics near open-circuit voltage.
2. The role of PEDOT:PSS layer in a multilayer hybrid TiO₂/polymer devices has been identified to arise from the characteristic changes on the morphology and the electrical properties. The optimum power conversion efficiency was observed with the 50 nm thick PEDOT:PSS layers. Improved performance with the aging was also observed in these solar cells.
3. In a multilayer hybrid TiO₂/P3HT solar cells the best dipping solvent with the optimized dipping conditions were studied. Dichlorobenzene was selected as the best dipping solvent with the optimized dipping concentration of 1 mg/ml and the optimized temperature 120 °C at the dipping time optimized at 2 h.
4. The TiO₂ incorporated with the grape fruit dye and the cyclometalated Ru based sensitizer MUJA1 promising in solar cell application. The performances of these solar cells are comparable to that made with the Z907 commercial sensitizer.
5. It has been found that a modified TiO₂ – Visible Light Responsive TiO₂ is promising n-type semiconductor for the DSSC applications. Compared with that of the commercial TiO₂. VLR-TiO₂ shows significant optical absorption features and revealed enhanced performance probably attributed to the high anatase content in VLR-TiO₂ which could enhance the dye adsorption and charge transport.

VI. References

1. IEA World Energy Outlook 2006-reports(updated)/Energy Bulletin (<http://www.energybulletin.net/node/22081>).
2. <http://www.beyondpeak.com/scenarios/becke.html>
3. International Energy Outlook 2008, US Energy Information Administration, <http://www.eia.doe.gov/oiaf/ieo/world.html>
4. Survey of energy Resources, World Energy Council, <http://www.worldenergy.org/wec-geis/publications/reports/ser/solar/solar.asp>
5. Photovoltaic Power systems programme, International Energy Agency,(www.iea-pvps.org)
6. M. A. Green, K. Emery, D. L. King, Y. Hishikawa, and W. Warta, *Prog. Photovoltaics*, 14, 455 (2006).
7. G. Li, V. Shrotriya, J. Huang, Y. Yao, T. Moriarty, K. Emery, and Y. Yang, *Nature Mater.*, 4, 864 (2005).
8. C. J. Brabec, N. S. Sariciftci, and J. C. Hummelen, *Adv. Funct. Mater.* 11, 15 (2001).
9. N. S. Sariciftci, L. Smilowitz, A. J. Heeger, and F. Wudl, *Science* 258, 1473 (1992).
10. I. Riedel , N. Martin , F. Giacalone , J.L. Segura , D. Chirvase , J. Parisi, and V. Dyakonov, *Thin Solid Film* 451,48 (2004).
11. Y. Kim, S. A. Choulis, J. Nelson, D. D. C. Bradley, S. Cook, and J. R. Durrant, *Appl. Phys. Lett.* 86, 063502 (2005).
12. J. Y. Kim, S. H. Kim, H. Lee, K. Lee, W. Ma, X. Gong, and A. J. Heeger, *Adv. Mater.* 18, 572 (2006).
13. T. Ishwara, D.D.C. Bradley, J. Nelson, P. Ravirajan, I. Vanseveren, T. Cleij, D. Vanderzande, L. Lutsen, S. Tierney, M. Heeney, I. McCulloch, *Appl. Phys. Lett.* 92, 053308 (2008).
14. P. Ravirajan, S. A. Haque, J. R. Durant, D. Poplavaskyy, D. D. C. Bradley, J. Nelson, *J. Appl. Phys.* 95, 1473 (2004).
15. P. Ravirajan, S. A. Haque, J. R. Durant, D. D. C. Bradley, J. Nelson, *Adv. Funct. Mater.* 15, 609 (2005).
16. P. Ravirajan, D. D. C. Bradley, J. Nelson, S. A. Haque, J. R. Durrant, H.J.P. Smit, J. M. Kroon, *Appl. Phys. Lett.* 86, 143101 (2005).
17. P. Ravirajan, A. Green, S.A. Haque, J.R. Durrant, D.D.C. Bradley, J. Nelson, *Proc. of SPIE.* 5520, 232-243 (2004).
18. P. Atienzar, T. Ishwara, B.N. Illy, M.P. Ryan, B.C.O'Regan, J.R. Durrant, J. Nelson, *J. Phys. Chem. Lett.* 1, 708–713 (2010).
19. L. Kavan, M. Gratzel, *Electrochim. Acta* 40, 643 (1995).
20. P. Ravirajan, "Characterization and optimization of hybrid polymer/ metal oxide photovoltaic devices", Ph.D. Thesis, University of London (2004).
21. P. Peumans and S. R. Forrest, *Appl. Phys. Lett.* 79, 126 (2001).
22. K. Takahashi, N. Kuraya, T. Yamaguchi, T. Komura, and K. Murata, *Sol. Energy Mater. Sol. Cells* 61, 403 (2000).
23. J. Nelson, J. Kirkpatrick, and P. Ravirajan, *Phy. Rev.* B69, 035337 (2004).
24. J. Nelson, *The Physics of Solar Cells*, Imperial College Press, London (2003).

25. E. A. Katz, D. Faiman, S. M. Tuladhar, J. M. Kroon, M. M. Wienk, T. Fromherz, F. Padinger, C. J. Brabec, and N. S. Sariciftci, *J. Appl. Phys.* 90, 5343 (2001).
26. I. Riedel, J. Parisi, V. Dyakonov, L. Lutsen, D. Vanderzande, and J. C. Hummelen, *Adv. Funct. Mater.* 14, 38 (2004).
27. D. Chirvase, Z. Chiguvare, M. Knipper, J. Parisi, V. Dyakonov, and J. C. Hummelen, *J. Appl. Phys.* 93, 3376 (2003)
28. M.Y. Song, K.J. Kim, D.Y. Kim, *Sol. Energy Mater. Sol. Cells* 85, 31-39 (2005).
29. Y.Y. Lin, C.W. Chen, T.H. Chu, Wei-Fang Su, Chih-Cheng Lin, Chen-Hao Ku, Jih-Jen Wub and Cheng-Hsuan Chenc, Nanostructured metal oxide/conjugated polymer hybrid solar cells by low temperature solution processes, *J. Mater. Chem.* 17 (2007) 4571–4576
30. J.G. Müller, J.M. Lupton, J. Feldmann, U. Lemmer, M.C. Scharber, N.S. Sariciftci, C.J. Brabec, U. Scherf, *PHYSICAL REVIEW B* 72 195208 (2005).
31. M.Senthilnathanan, D. P. Ho, S. Vigneswaran, H. H. Ngo, H. K. Shon, *Separation and purification technology*, 75 (2010).
32. H. Tang, K. Prasad, R. Sanjinbs, P. E. Schmid, and F. Levy, *J. Appl. Phys.* 75, 2042-2047 (1994).

viii) Problems if any encountered during the implementation of the project

There was delay in purchase a glove box in the later part of the project within the budget, but it has been short it after granting the extended period of time for the project.

ix) Major findings and follow up activities

The device structure we adopted in connection with the hybrid TiO₂/polymer solar cells offered very high power conversion efficiency. However the reproducibility was being a big problem in these solar cells most probably due to the properties of the backing layer. Hence priority would be given to the fabrication of these solar cells while controlling the properties of the backing layer. The modification of the TiO₂/polymer interface by the novel sensitizers like Muja 1 is also expected to be fulfilled.

Section 4

Impact of Research results:

i. Relevance of results achieved to scientific advancement

As the energy crisis has nowadays felt as a global threat quest for cheap energy has also become science's major pre-occupation. The field of polymer solar cells has attracted researchers all over the world who are contributing to make advancements in this field. This project made significant contribution for the present understanding of polymer based solar cells.

ii. Relevance of results achieved to national/socio-economic development

The steep rise in the oil prices in the recent past has created a great burden to the economy in supplying of the fossil fuel energy sources without fluctuations. In order to mitigate the burden the available options are the utilization of renewable energy sources and efficiency improvement in the current use. Energy security has thus identified as an important factor for the socio economic development policy framework of Sri Lanka. In order to achieve the objectives articulated in the economic policy framework supplying of reliable, affordable and clean energy is extremely important in this regard to ensure sustainable socio-economic development.

iii. Dissemination of project output

The output of this work will be much useful to the organic based solar cells research community as well as investor for plastic solar cells. The results of this project have been presented in international (indexed and refereed) and local journals as well as local scientific meetings. To make a public awareness about the solar energy and solar cells we wrote an article titled "Solar energy is the most appropriate energy source for Sri Lanka" which appeared in the "Uthayan" local newspaper.

Section 5

Miscellaneous

- i. List of major equipment acquired during the project period and their functionality**
- ii. List of publications/communications arising from the project and/presentations made at seminars, workshops etc.**

Major equipment

Glove box

List of indexed Journal Papers

1. Effect of temperature and light intensity on the performance of polymer/fullerene solar cells with titanium dioxide nanolayers, **S. Sarathchandran**, K.Haridas, Y.Kim, P. Ravirajan, J. Nanoelectronics Optoelectron. vol. 5, 243-246(2010).

2. Role of PEDOT: PSS underlayer on the performance of nanocrystalline TiO₂/ P3HT multilayer solar cells, **S.Sarathchandran**, K.Prashanthan and P.Ravirajan, J. Nanoelectron. Optoelectron 6(3), 272-276 (2011).

List of conference proceedings

3. Enhancing the performance of Hybrid TiO₂/polymer multilayer Solar Cells by modifying theTiO₂/polymer interface by Single Wall Carbon Nanotube (SWNT), K. Balashangar, T. Jaseetharan, **S. Sarathchandran** and P. Ravirajan, International Conference on Solar Energy Materials, Solar cells and Solar Energy Applications (SOLAR ASIA- 2011) 258 (2011).
4. Visible light responsive nanocrystalline TiO₂ for dye sensitized solar cells, B. Kajitha, **S. Sarathchandran**, M. Senthilnathanan and P. Ravirajan, International Conference on Solar Energy Materials, Solar cells and Solar Energy Applications (SOLAR ASIA- 2011) 253 (2011).
5. Novel Cyclometallated Ruthenium dye sensitizer for nanocrystalline TiO₂ based Solar cells, M.Senthilnathanan, **S.Sarathchandran** John.M.Brown, S.Sivaraya and P.Ravirajan,Proceedings of the International conference on “Advances in Continuum mechanics,Nanoscience and Nanotechnology: Dedicated to Professor Munidasa P. Ranaweera”, University of Peradeniya, Sri Lanka, September 26-27, 2008, Pages 240-245.

List of abstracts (International Conferences)

6. Utilisation of Plant pigments in Dye-Sensitised Nanoporous TiO₂ SolarCells, T.Jaseetharan, **S.Sarathchandran**, K..Jeyakanthan, M.Senthilnathanan, S.Sivaraya and P.Ravirajan,17th International Conference on Photochemical Conversion and Storage of Solar Energy, Sydney, Australia, July 27- August 01, 2008.
7. Cost efficient solar cells based on nanocrystalline titanium oxides and natural dye that extracted from plants, **S.Sarathchandran**, K.Jeyakanthan,M. Senthilnathanan^b and P.Ravirajan, IFS/OPCW Workshop, 7-10 December 2009.
8. Influence of dipping solvent in improving polymer infiltration in nanocrystalline TiO₂/polymer solar cells, V. Jathushan, **S. Sarathchandran** and P. Ravirajan, International Conference on Solar Energy Materials, Solar cells and Solar Energy Applications (SOLAR ASIA 2011).
9. Influence of dipping solvent in improving polymer infiltration in nanocrystalline TiO₂/polymer solar cells, V. Jathushan, **S. Sarathchandran** and P. Ravirajan, International Conference on Solar Energy Materials, Solar cells and Solar Energy Applications (SOLAR ASIA 2011)

List of abstracts (Local Scientific meeting)

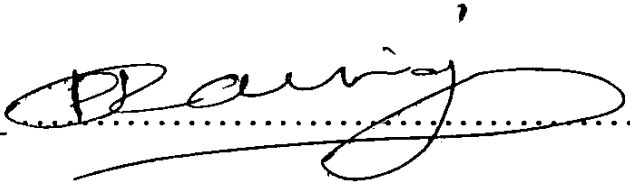
10. Natural plant pigments to serve as Dye-Sensitized Nanoporous TiO₂ Solar Cells T.Jaseetharan, **S.Sarathchandran**, K.Jeyakanthan, M.Senthilnathanan, S.Sivaraya and P.Ravirajan, *National Conference on Advanced Materials for Emerging Technologies (NCAMET 2007)* Peradeniya ,21-22 July 2007.
11. Effect of self-assembling dipole molecules on the performance of TiO₂/Polythiophene:fullerene solar cells, **Selvaratnam Sarthchandran** Tharsani Amirthalingam and Punniamoorthy Ravirajan, *National Conference on Advanced Materials for Emerging Technologies (NCAMET 2007)* Peradeniya, 21-22 July 2007.
12. T.Jaseetharan,K. Jeyakanthan,S.Satchithanathan,M. Senthilnathanan ,**S. Sarathchandran** S. Sivaraya and P. Ravirajan,Solid state solar cells made from nanocrystalline TiO₂ with plant pigments as sensitizers, Proceeding of JSA, 2008.


Articles

13. Co authored an article titled “An appropriate alternative source for electricity needs of Jaffna peninsula”-Centenary souvenir, St.Hentry’s college, Ilavalai, pages 142-151.

Section 6 Summary statement of Expenditure

Personal	898,333.33
Miscellaneous	2,000.00
Glove box	777,038.13
Custom duty & clearing charges	347,071.00
Total	2,024,442.46

Signature of the grantee and Head/Physics: 

Signature of the Dean/Faculty of Science :- 

Signature of the Vice-Chancellor/University of Jaffna:- 



Role of Poly(Ethylenedioxythiophene)/Poly(Styrene Sulphonate) on the Performance of Nanocrystalline Titanium Dioxide/Poly(3-Hexylthiophene) Polymer Solar Cells

S. Sarathchandran, K. Prashanthan, and P. Ravirajan*

Department of Physics, University of Jaffna, Jaffna, JA 40 000, Sri Lanka

Hybrid nanocrystalline titanium dioxide (TiO₂)/polymer solar cells draw intense interest due to the potential advantages of nanocrystalline TiO₂. The poly(styrenesulfonate)-doped poly(ethylenedioxy thiophene) (PEDOT:PSS) layer spin-coated below the top electrode in these solar cells had shown enhanced performance in previous studies, which motivated to explore the dependence of the thickness of the PEDOT:PSS layer on its performance. This study focused on the characterization of solar cells fabricated with poly(3-hexylthiophene) (P3HT) polymer with a silver electrode and different PEDOT:PSS layer thicknesses, in the dark and under AM 1.5 stimulated illumination with the intensity varying from 10 to 100 mW/cm². The variations in the photovoltaic parameters, particularly the open-circuit voltage, proved that the PEDOT:PSS layer significantly affects the photovoltaic parameters through the characteristic changes in the morphology as well as the electrical properties. Discussed herein is the possible influence wielded by the thickness of the PEDOT:PSS layer on different factors, such as the series and shunt resistances, the mode of recombination, the reduction of the energy barrier, and the diffusion of silver. The optimum power conversion efficiency was observed for the as-prepared devices with 50-nm-thick PEDOT layers. The optimum power conversion efficiency, however, shifted to that corresponding to the 80 nm thick PEDOT:PSS layer about 30 weeks after the fabrication. A sublinear variation of the short-circuit current density with the intensity was found in the aged cells with relatively lower PEDOT:PSS layer thicknesses, supporting the view of dominant recombination contributed from bimolecular recombination in the cells with lower PEDOT:PSS thicknesses. The significantly increased open-circuit voltage and the more stable current density in the aged devices are the main causes of the improved performance of the cells generally with above 60 nm-thick PEDOT:PSS layers. These, along with the long-term stability found in the cells with reasonably thick PEDOT:PSS layers, may be a figure of merit, most probably attributable to the comparatively minimized diffusion of silver nanoparticles.

Keywords: Solar Cells, PEDOT:PSS, Polymer, TiO₂, Thickness, Photovoltaic Device.

1. INTRODUCTION

Solar cells utilizing molecular materials are currently under intensive research as potential replacements for the traditional microcrystalline solar cells, because of their relative ease of fabrication with cost-efficient methods. A class of solar cells fabricated with blends of polymers and fullerene derivatives at nanoscale has yielded the highest efficiency among the organic solar cells. The use of fullerenes as electron acceptors has some disadvantages, however, such as the phase segregation of

the components during aging, and the relatively poor photostability. Stable metal oxides such as TiO₂, ZnO, and SnO₂ are promising as alternative electron acceptors that could offer good electron transport properties, fabrication via facile techniques, nontoxicity, and heterojunction morphology control.¹⁻⁸ These hybrid solar cells fabricated with metal oxide and polymer can further assume the advantages of both types of materials.^{8,9} The hybrid TiO₂/polymer solar-cell system is more attractive as the titania templates can be made with continuous pores with the size matching the exciton diffusion length, which improves exciton harvesting. The performance of these hybrid TiO₂/polymer solar

*Author to whom correspondence should be addressed.

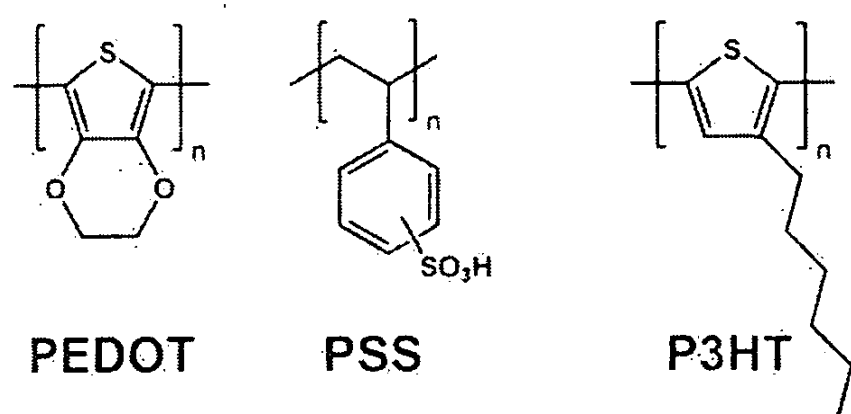


Fig. 1. Chemical structure of poly(ethylenedioxy thiophene: poly(styrenesulfonate))-(PEDOT:PSS) and poly(3-hexylthiophene) (P3HT).

cells, however, are still lower than that of the reported best polymer:fullerene solar cells mainly due to the limited photogeneration rate and the quality of the interfaces.³ Several attempts to modify the TiO₂/polymer interface have been made and reported.¹⁰ The polymer/top-electrode interface modified with poly(styrenesulfonate)-doped poly(3,4-ethylenedioxythiophene) (PEDOT:PSS) has also been determined to improve the performance of the TiO₂/polymer solar cells.^{3,4,10,11} The PEDOT:PSS underlayer has been found to enhance the hole collection by establishing ohmic contact with the polymer layer¹² while serving as an electron-blocking layer. Furthermore, the degraded current density-voltage (*J-V*) characteristics owing to the energy barrier at the polymer/top hole-collecting metal electrode were reported to have been reduced by the introduction of the PEDOT:PSS underlayer.³⁻⁵ The PEDOT:PSS underlayer can also serve as a protective layer from the damages that can be caused by metal penetration during thermal evaporation, which may enhance the exciton quenching near the interface. With this background, a study related to the quality of the PEDOT:PSS layer in the hybrid TiO₂/polymer solar cells is important for optimizing the performance of the layer.

The present study focused on the effect of the thickness of the PEDOT:PSS layer on the performance of the hybrid TiO₂/P3HT multilayer solar cell fabricated with a silver top electrode. The possible influence of the PEDOT:PSS layer thickness on several factors, including the reduction of the interfacial energy barrier, recombination, compatibility between the interface layers, and the diffusion of the silver nanoparticles, are discussed in this paper.

2. EXPERIMENTAL DETAILS

Indium-tin-oxide-(ITO)-coated glass substrates (25 Ω/cm²) were cleaned using acetone and isopropyl alcohol, and were then annealed to remove any organic residue. The precursor solution that was used to deposit the dense TiO₂ nanolayer, prepared as described in Ref. [13], was sprayed onto the cleaned ITO-coated glass substrates and were subsequently sintered at 450 °C for 30 min. This dense TiO₂ layer prevents direct contact between

poly(3-hexylthiophene) (P3HT) and the ITO-coated glass substrate, which would short-circuit the device. The porous nanocrystalline TiO₂ film was deposited on the dense TiO₂ layer by spin-coating the diluted TiO₂ paste purchased from Dysol (Australia), and was then sintered at 450 °C for 30 min. After allowing sufficient time for the substrates to cool down, they were dipped in the P3HT (purchased from Merck Chemicals Ltd.) solution in 1,2 dichlorobenzene for 24 h. After being blown with nitrogen gas, they were soft-baked at 50 °C for 5 min, and the P3HT layer (~50 nm thick) was spun on this substrate.

To fabricate the PEDOT:PSS underlayer, the aqueous solution of PEDOT:PSS (BAYTRON) after filtering with a 0.45-μm filter was heated at 90 °C for 5 min. It was then spin-coated at different spin rates, ranging from 1050 to 10100 rpm, onto the P3HT layer. The samples were again baked at 100 °C for 5 min in a nitrogen-filled, home-built annealing box. Solar cells were fabricated through the deposition of a silver film on the PEDOT:PSS layer under vacuum, below 10⁻⁵ Torr, in the chamber of the thermal evaporator. A dot of silver paint was applied on top of this silver film and on the ITO bottom electrode for better contact, and was subsequently annealed at 120 °C in a nitrogen environment.

The *J-V* characteristics were obtained with a Keithley 2400 Source Measure unit. The cells were characterized in the dark and under illumination with a solar simulator (SCIENCETECH) at varying intensities.

3. RESULTS AND DISCUSSION

The *J-V* characteristics of the hybrid TiO₂/P3HT multilayer devices with different PEDOT:PSS thicknesses characterized in the dark and under AM 1.5 simulated illumination with a typical intensity of 70 mW/cm² are shown in Figures 2(a and b), respectively.

The forward-biased dark current of the nanostructured TiO₂/polymer solar cells with varying PEDOT:PSS underlayer thicknesses showed a significant increase compared to those without such layer, in accord with the previous studies.^{3-5,10} The dark-current rectification ratio, however, was observed to decrease when the thickness of the PEDOT:PSS layer was continuously increased up to about 80 nm, but was observed to increase when the thickness exceeded 90 nm. The PEDOT:PSS layer whose thickness exceeded 100 nm, however, was peeled off from the substrate. For this reason, the analysis was restricted to the moderately thick PEDOT:PSS layers, although techniques like encapsulation may remedy the aforementioned problem identified with thick PEDOT:PSS layers.

The previous reports attribute the drop in serial resistance, the subsequent increase in the dark current and current under illumination, the absence of a distorted feature near the open-circuit voltage, and the minimal reduction in the open-circuit voltage to the reduction of the

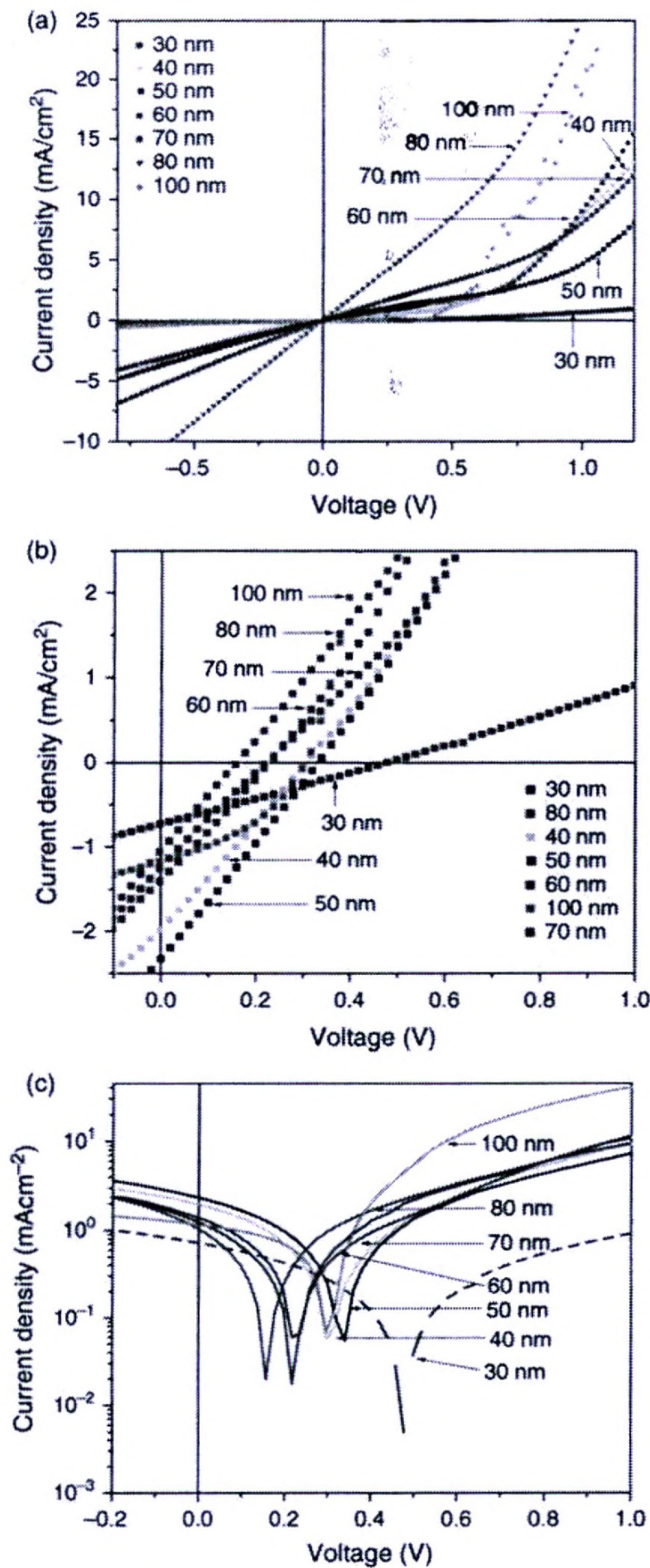


Fig. 2. J - V characteristics of the hybrid TiO₂/P3HT multilayer solar cells with different PEDOT thicknesses (a) in the dark and (b) under AM 1.5 illumination with a solar simulator with an intensity of 70 mW/cm². (c) Replotted in semilogarithmic scale for better observation of the change in the open-circuit voltage.

polymer/metal electrode energy barrier resulting from the inclusion of a PEDOT:PSS layer.⁴⁻⁷ In the present study, the open-circuit voltage (V_{OC}) started to fall continuously, reaching the minimum level, and seemed to increase again for the cells with reasonably thick PEDOT:PSS layers (~100 nm), as can be seen in Figure 2. The short-circuit current density (J_{SC}) was maximized with the around 50 m PEDOT:PSS layer thickness. The optimum power

conversion efficiency was observed with the about-50-nm-thick PEDOT:PSS layer, as shown in Figure 3. The comparatively inferior power conversion efficiencies shown by the 70- and 80-nm-thick PEDOT:PSS layers of the solar cells mainly resulted from the poor V_{OC} .

It should be noted that the power conversion efficiency was not absolutely optimized but only entailed relative variation with the PEDOT:PSS thickness in this work because some of the steps, such as dye dipping prior to dipping in the polymer solution, were skipped in this study, for simplicity. Similarly, the identical steps followed in the preparation of the dense TiO₂ hole-blocking layer, which is known as vital for the optimization of the performance of the nanocrystalline TiO₂/P3HT polymer solar cells, removed the influence of the quality of the dense TiO₂ hole-blocking layer on the results of this comparative study.

A number of factors associated with the PEDOT:PSS layer will be identified to explain the PEDOT:PSS-controlled photovoltaic parameters. The morphology-related factors, such as surface roughness, compactness, distribution of voids, uniformity, and quality of adherence to the surface of P3HT, possibly influence the polymer/metal electrode energy barrier, series and shunt resistance, and recombination mode, and may thereby control the photovoltaic parameters. Better compatibility, which leads to a reduced energy barrier, as has already been confirmed in the previous studies,^{5,6} cannot be expected to be attained with very thin PEDOT:PSS layers. The reduction of the surface roughness and the filling of voids may contribute positively to the reduction of the series resistance with increasing thickness. It is reasonable to expect a saturated reduced-barrier level, and its consequence of enhancing the charge collection, due to the aforementioned morphology-related factors, up to a certain thickness. When the thickness increased to a certain extent,

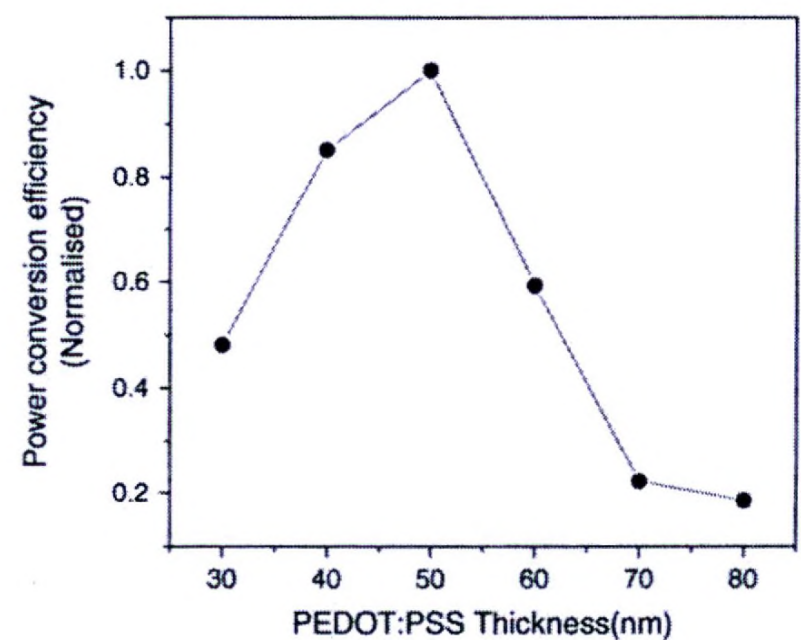


Fig. 3. Normalized power conversion efficiency of the hybrid TiO₂/P3HT multilayer solar cells with different PEDOT:PSS thicknesses (30, 40, 50, 60, 70, and 80 nm) under stimulated illumination with 70 mW/cm² light intensity.

the series resistance tended to increase, mainly receiving contributions from the layer resistance itself. Furthermore, the layer resistance obtains importance due to the hygroscopic nature of the PEDOT:PSS layer, which decreases the conductivity.

The shunt resistance, on the other hand, is a measure of the inverse of the slope of the J - V curve near J_{SC} . The shunt resistance in this analysis showed an initial steep fall followed by a gentle decrease and another steep increase with increased PEDOT:PSS thickness, reflecting the trend shown by V_{OC} . Noncompact and nonuniform films probably lead to pinholes acting as shunt pathways that degrade the performance. The effect of the diffusion of silver nanoparticles towards P3HT through the PEDOT:PSS layer is not well understood, but if the diffusion reaches a critical stage, the increased shunt pathways will definitely decrease the shunt resistance.

The PEDOT:PSS layer may also influence the charge carrier recombination, which generally depends on the macroscopic film properties, such as the sizes and shapes of the cells and the nanoscale phase-separated regions, percolation paths,¹⁴ molecular arrangement, and traps. In the cells with too thin or too thick PEDOT:PSS layers, a slower rate of hole collection can be expected compared to the rate of generation, which in turn makes the recombination and/or space-charge-limited current dominant. The effect of the recombination and/or space-charge-limited current will become even more dominant in the thin PEDOT:PSS layer cells due to the inefficient electron-blocking function carried out by the thin PEDOT:PSS layer.

Another important observation is the aging effect, which affects the performance of the solar cells in a somewhat unexpected manner. The optimum power conversion efficiency shifted to that corresponding to the 80-nm-thick PEDOT:PSS layer about 30 weeks after the fabrication. The significantly increased V_{OC} and the more stable J_{SC} in the aged devices were the main causes of the improved performance of the cells with generally more-than-60-nm-thick PEDOT:PSS layers. These, along with the long-term stability found in the cells with reasonably thick PEDOT:PSS layers, may be merits most probably attributable to the comparatively minimized diffusion of silver nanoparticles.

Both the aged and the as-prepared cells depicted the same trend of variation in J_{SC} and V_{OC} when exposed to varying light intensity. The degree of variation, however, was lower in the as-prepared cells. Figure 4 shows the variation of the J_{SC} and V_{OC} of the aged cells with varying light intensity.

Figure 4(a) shows the significant increase in the V_{OC} at a particular intensity compared to the as-prepared cells. The sublinear variation of J_{SC} with the intensity could be seen in the aged cells with relatively lower PEDOT:PSS layer thicknesses, supporting the view of the dominant recombination contributed from the bimolecular recombination in

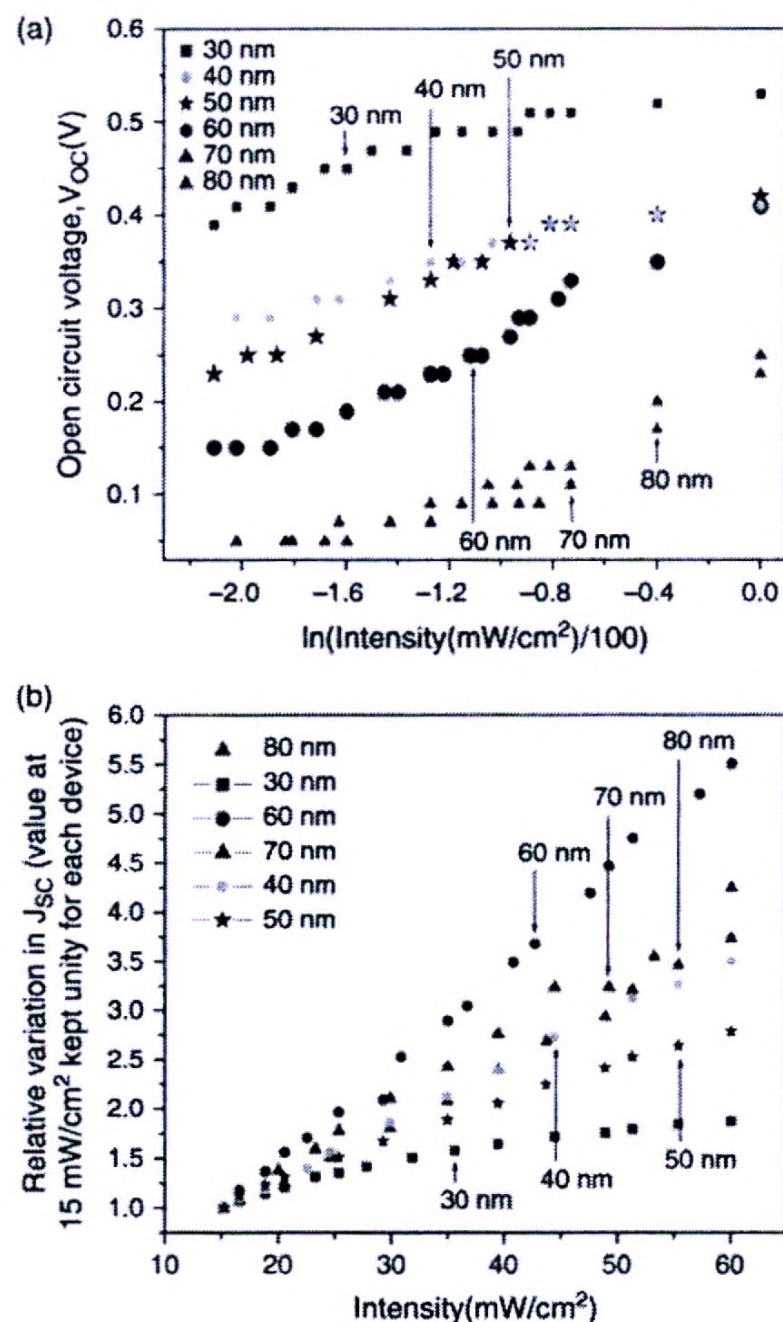


Fig. 4. Variation in the (a) open-circuit voltage with \ln (intensity) and (b) short-circuit current density with the intensity relative to a very low intensity of 15 mW/cm^2 of the ITO/dense TiO_2 layer/porous TiO_2 layer/P3HT/PEDOT:PSS/Ag cells with varying PEDOT:PSS thicknesses (x nm) after 30 weeks elapsed time (kept under vacuum).

these cells with lower PEDOT:PSS layer thicknesses. The possibility, however, that the space-charge-limited current resulted in this sublinear variation cannot be ruled out.

4. CONCLUSION

It was found that the photovoltaic parameters controlled by the thickness of the PEDOT:PSS layer in a multi-layer hybrid TiO_2 /polymer cell can be attributed to the characteristic changes in the morphology and electrical properties, including the series and shunt resistances, the reduction of the energy barrier, the diffusion of the silver top metal contact, and the recombination mode. The optimum power conversion efficiency was observed with the 50-nm-thick PEDOT:PSS layers. Improved performance with aging was observed, however, in the cells with much thicker PEDOT:PSS layers, which is attributed to the more stable current density in these cells and the significant increase in the open-circuit voltage, which had been found to be very low in the as-fabricated cells.

Acknowledgment: PR and SS acknowledge the National Research Council and National Science Foundation, Sri Lanka for their financial assistance, respectively.

References and Notes

1. T. Ishwara, D. D. C. Bradley, J. Nelson, P. Ravirajan, I. Vanseveren, T. Cleij, D. Vanderzande, L. Lutsen, S. Tierney, M. Heeney, and I. McCulloch, *Appl. Phys. Lett.* 92, 053308 (2008).
2. P. Ravirajan, S. A. Haque, J. R. Durant, D. Poplavaskyy, D. D. C. Bradley, and J. Nelson, *J. Appl. Phys.* 95, 1473 (2004).
3. P. Ravirajan, S. A. Haque, J. R. Durant, D. D. C. Bradley, and J. Nelson, *Adv. Funct. Mater.* 15, 609 (2005).
4. P. Ravirajan, D. D. C. Bradley, J. Nelson, S. A. Haque, J. R. Durrant, H. J. P. Smit, and J. M. Kroon, *Appl. Phys. Lett.* 86, 143101 (2005).
5. P. Ravirajan, A. Green, S. A. Haque, J. R. Durrant, D. D. C. Bradley, and J. Nelson, *Proc. of SPIE* 5520, 232 (2004).
6. P. Atienzar, T. Ishwara, B. N. Illy, M. P. Ryan, B. C. O'Regan, J. R. Durrant, and J. Nelson, *J. Phys. Chem. Lett.* 1, 708 (2010).
7. J. Bouclé, H. J. Snaith, and N. C. Greenham, *J. Phys. Chem.* 114, 3664 (2010).
8. S. Sarathchandran, K. Haridas, Y. Kim, and P. Ravirajan, *J. Nanoelect. Optoelectron.* 5, 243 (2010).
9. W. J. E. Beek, M. W. Wienk, and R. A. J. Janssen, *Adv. Funct. Mater.* 16, 1112 (2006).
10. B. Johaan, P. Ravirajan, and J. Nelson, *J. Mater. Chem.* 17, 3141 (2007).
11. M. Y. Song, K. J. Kim, and D. Y. Kim, *Sol. Energy Mater. Sol. Cells* 85, 31 (2005).
12. G. Khrypunov, S. Bereznev, A. Meriuts, G. Kopach, N. Kovtun, and N. Deyneko, *Physics and Chemistry of Solid State T. II*, 249 (2010).
13. L. Kavan and M. Gratzel, *Electrochim. Acta* 40, 643 (1995).
14. J. G. Müller, J. M. Lupton, J. Feldmann, U. Lemmer, M. C. Scharber, N. S. Sariciftci, C. J. Brabec, and U. Scherf, *Physical Review B* 72, 195208 (2005).

Received: 20 April 2011. Accepted: 8 June 2011.



Effect of Temperature and Light Intensity on the Performance of Polymer/Fullerene Solar Cells with Titanium Dioxide Nanolayers

S. Sarathchandran¹, K. Haridas^{1,2}, Y. Kim³, and P. Ravirajan^{1,*}

¹Department of Physics, University of Jaffna, Jaffna, Sri Lanka

²Department of Physics, University of Bristol, UK

³Department of Chemical Engineering, Kyungpook National University, South Korea

In this work, alternative architecture for polymer/fullerene solar cells has been explored using titanium dioxide nanolayers which invert the polarity of the cell and may relax the necessity to have a hole-collecting buffer layer poly(styrene sulfonate)-doped poly(ethylene dioxy-thiophene) (PEDOT:PSS). This work particularly focuses on the performance of the inverted devices with dense TiO₂ nanolayers as a function of temperature, illumination intensity and time. We find that both temperature and illumination intensity slightly influence the power conversion efficiency of devices with the PEDOT:PSS layer. However, the inverted solar cells without the PEDOT:PSS layer showed very different characteristics regarding the power conversion efficiency which increased significantly with the operating temperature from 30 °C to 65 °C. This was attributed to a consequence from the strong and positive temperature dependence of open-circuit voltage which may be due to a “kink” in the current–voltage characteristics near the open-circuit voltage.

Keywords:

1. INTRODUCTION

Solar cells made from conjugated polymers and fullerene derivatives are promising candidates for photovoltaic conversion due to their mechanical flexibility, light weight, ease of processability and low cost fabrication of large areas.^{1–5} Of various combinations, devices made using blend films of poly(3-hexylthiophene) (P3HT) and soluble fullerene derivative ([6,6]-phenyl-C₆₁-butyric acid methyl ester) (PCBM) deliver reproducible high efficiency >4%, which typically have poly(styrenesulfonate)-doped poly(ethylenedioxythiophene) (PEDOT:PSS) as a hole-collecting buffer layer. However, these solar cells suffer from degradation due to the PEDOT:PSS layer which oxidizes the active material. Alternative architectures for P3HT:PCBM solar cells, which relax the necessity for the PEDOT:PSS layer, are thus become a preferred option.

The P3HT:PCBM incorporated with nanolayers of metal oxides is one such alternative. In these solar cells, the polarity is reversed as compared to the conventional P3HT:PCBM solar cells and are referred to as inverted solar cells. When comparing the P3HT:PCBM solar cell

with the hybrid TiO₂/polymer solar cells, the lower interfacial site is a disadvantage for the latter, but the slower recombination is an advantage.⁶ It may be therefore possible to have the merits of both of these TiO₂:P3HT and P3HT:PCBM in the TiO₂ incorporated P3HT:PCBM inverted solar cell. The charge carrier recombination may be even slower in the inverted solar cells because of the two-step charge carrier separation. Hole blocking is another added advantage offered by the dense TiO₂ nanolayer which enhances the charge transport in the inverted solar cells. Moreover, the TiO₂ nanolayer is an excellent electron transporting non-toxic material which possesses potential for controlling interface morphology, mechanical and chemical stability.⁷

In this work we study the influence of the temperature, illumination intensity and time on the solar cell parameters of the TiO₂/PCBM:P3HT inverted solar cells with or without the PEDOT:PSS nanolayer. A striking feature with the inverted devices without the PEDOT:PSS layer is that the power conversion efficiency depends on a distorted feature in the current–voltage characteristics near the open-circuit voltage. We discuss the possible origin of this so-called “kink” and how it controls the power conversion efficiency.

*Author to whom correspondence should be addressed.

2. EXPERIMENTAL DETAILS

Indium-tin oxide (ITO)-coated glass substrates ($\sim 25 \Omega/\text{cm}^2$) were first cleaned several times thoroughly in acetone and isopropanol and then annealed to remove any organic residue. They were then blown with nitrogen gas. To prepare the dense TiO_2 nanolayer, precursor solution was prepared using titanium isopropoxide and acetylacetone as described in the Ref. [8] for the hole blocking purpose. A dense layer of TiO_2 was made on the ITO glass using the spray pyrolysis technique and sintered at 450°C for 30 minutes. Blend solutions were prepared with P3HT and PCBM, purchased from Merck Chemicals Ltd, with a 1:1 weight ratio in chlorobenzene at a solution concentration of 25 mg/ml. These solutions were vigorously stirred for more than 24 hours to maximize mixing. The blend solution of P3HT:PCBM was then spin-coated onto this substrate (1250 rpm) after which the films were annealed at 120°C for 120 minutes in an N_2 environment. Some of the devices were with PEDOT:PSS layer onto this substrate. To make the PEDOT:PSS layer, the aqueous solution of PEDOT:PSS (Baytron) after filtering through a $0.45 \mu\text{m}$ filter was heated at 90°C for 5 minutes. It was then spin-coated at 4000 rpm. The substrates were again baked at 100°C for another 5 minutes in the nitrogen environment. Finally, gold top contact was made by thermal evaporation at a pressure better than 5×10^{-6} Torr. After that they were annealed at 120°C for 10 minutes in a home-built annealing box filled with nitrogen. The current-voltage (I - V) measurements (using a Keithley 2400 source meter) of these photovoltaic devices were carried out in a closed cycled cryostat using He gas and in a furnace both in the dark and illumination under white light.

3. RESULTS AND DISCUSSION

Figure 1 shows that the current density-voltage (J - V) characteristics of an inverted device without PEDOT:PSS (ITO/dense TiO_2 /PCBM:P3HT/Au) in a temperature range varying from 30°C to 75°C prominently differ from the other solar cells in that a 'kink' exhibited in the vicinity of the open-circuit voltage, V_{OC} . In this vicinity, the slope of the J - V curve for voltages less than V_{OC} ($V_{\text{OC}} - \Delta V$, infinitesimal ΔV is assumed to be positive) is very sensitive to both the temperature and intensity, compared to for voltages greater than V_{OC} . It should be noted that the inverse of the slope represents series resistance and it follows that the series resistance shifted to a higher value when the applied voltage passed the V_{OC} from $V_{\text{OC}} - \Delta V$ to $V_{\text{OC}} + \Delta V$. The kink cannot be claimed as specific to these types of devices only, but has already been observed in hybrid metal oxide/polymer solar cells and multilayer molecular film copper phthalocyanine (CuPc)/C60 solar cells^{9,10} when there is an energy step at polymer/top contact or bottom contact/copper phthalocyanine (CuPc),⁹

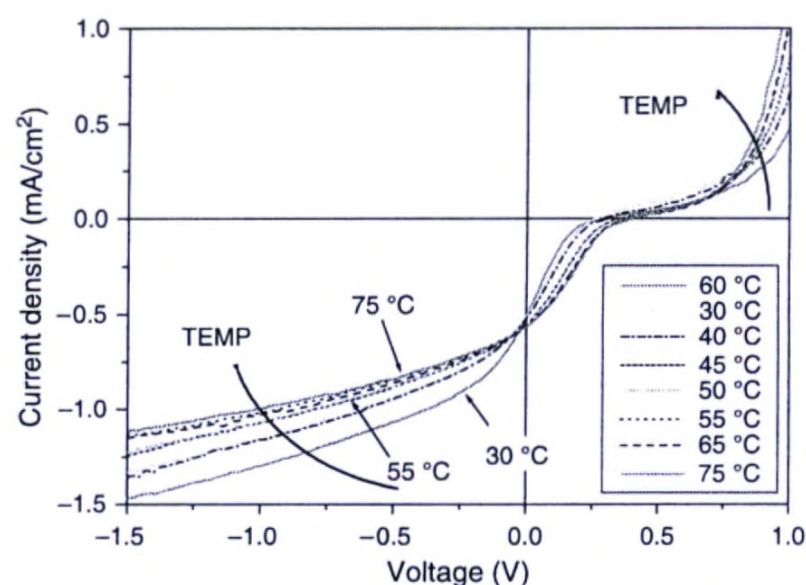


Fig. 1. Current-voltage characteristics of ITO/dense TiO_2 /PCBM:P3HT/Au device at different temperatures and under white light illumination of intensity of 10 mW cm^{-2} .

respectively. A modeling study confirmed that the kink in the current-voltage curve close to the open-circuit may be due to the presence of large interfacial energy steps or low carrier mobilities and a reduction of the open-circuit voltage and crossing of the light and dark current curves when interfacial recombination is strong.¹¹ However, the power conversion efficiency, controlled to a considerable extent by the kink, is the main outcome that distinguishes our present study from earlier observations and studies. Moreover, this kink effect becomes dominant with an increase in temperature or intensity.

Figure 2 shows that the power conversion efficiency of the inverted PCBM:P3HT solar cells with a TiO_2 nanolayer significantly increases (nearly a factor of 3) with temperatures in the range of 30°C to 65°C . The strongly temperature-dependent open-circuit voltage with a positive temperature coefficient in the temperature range of 30°C - 65°C is the major underlying reason for this strange behavior in terms of the power conversion efficiency. The very similar trends of temperature responses in relation to power conversion efficiency and the open-circuit voltage (as depicted in Figs. 2 and 3) further support that

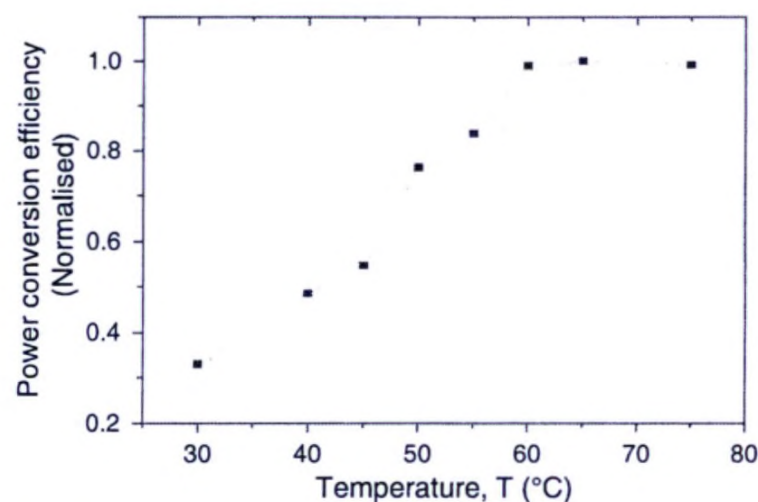


Fig. 2. Normalized power conversion efficiency of ITO/HBL/PCBM:P3HT/Au at different temperatures.

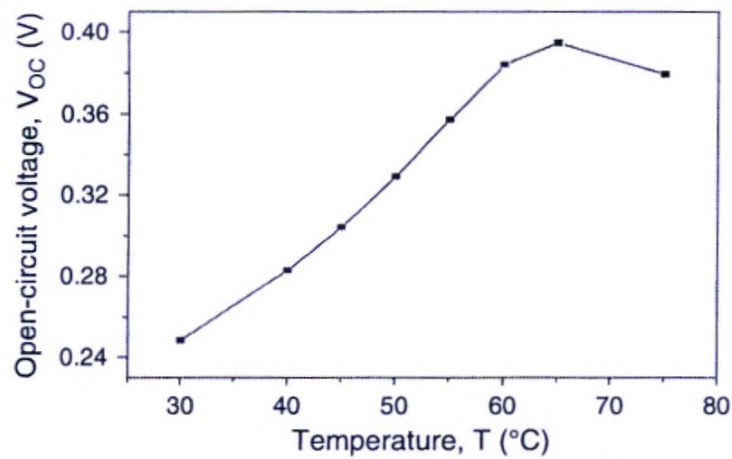


Fig. 3. Open-circuit voltage of the inverted solar cell, ITO/dense TiO_2 /PCBM: P3HT/Au.

the power conversion efficiency mostly relies on the open-circuit voltage.

For a solar cell that behaves as a non-ideal diode, current density J is given approximately by

$$J = J_{SC} - J_0 [\exp(eV/mkT) - 1] \quad (1)$$

Where J_0 is the dark saturation current density, m is the ideality factor, k is Boltzmann's constant and T the temperature.¹² Open-circuit voltage, V_{OC} , is then related to short-circuit current, J_{SC} through

$$V_{OC} = \frac{mkT}{e} \ln \left[\frac{J_{SC}}{J_0} \right] \quad (2)$$

Substituting for J_0 one could obtain the expression¹¹

$$V_{OC} = a - bT \quad (3)$$

where a and b are constants involving the intrinsic parameters of the active material.

The linear decrease of V_{OC} with temperature as governed by Eq. (3) was observed in several structures. A linear decrease of V_{OC} with average temperature coefficient $dV_{OC}/dT = -(1.40-1.65) \text{ mV}/^\circ\text{C}$ has been reported for typical PCBM/P3HT cells with PEDOT:PSS buffer layer within a temperature range of 30 °C to 60 °C.¹³ However, V_{OC} of the inverted solar cell shows almost linear increase with temperature, having an average temperature coefficient $dV_{OC}/dT = +6.9 \text{ mV}/^\circ\text{C}$ violating the non-ideal diode model.

At V_{OC} dark current is compensated by the current under illumination and hence making the zero photocurrent. If the kink effect was not present, there would be no discontinuity of the slopes of $J-V$ curve at the V_{OC} which leads to the decrease in V_{OC} similar to the conventional devices, which is not the real case. This supports the kink-controlled V_{OC} .

It has been reported in the literature about the strong temperature dependence of J_{SC} of the polymer: fullerene solar cells.¹³⁻¹⁵ In our case, J_{SC} exhibits an increasing trend on temperature, attains the maximum around 65 °C and falls down with the further increase in temperature. The

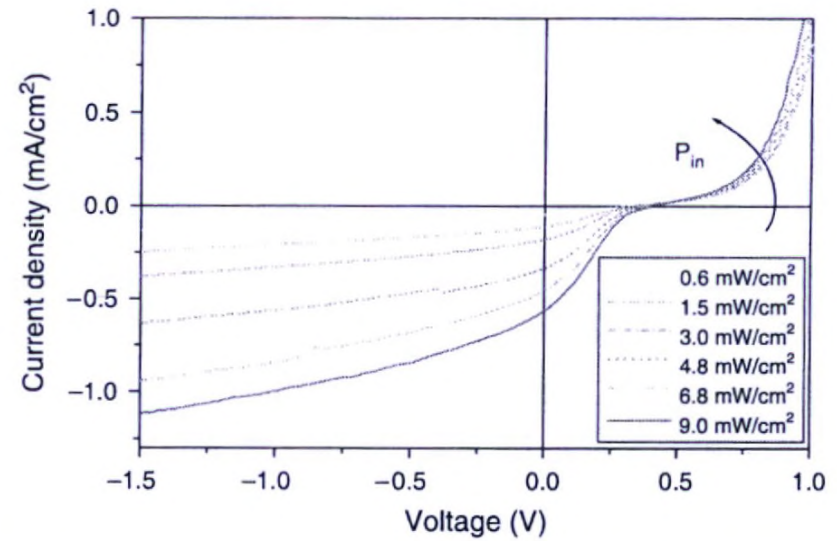


Fig. 4. Current density–voltage characteristics of ITO/HBL/PCBM: P3HT/Au at a temperature of 65 °C under different white light intensities ranging from 0.6 mW/cm^2 to 9 mW/cm^2 .

fill factor of the polymer: fullerene solar cells is usually low compared to the other structures because of the possible shunt pathways present due the blend nature. In the inverted solar cells, the FF becomes even lower because of the kink.

Figure 4 shows the current density–voltage characteristics of the inverted solar cell at a temperature of 65 °C under different low light intensities. In this intensity range, the scaling exponent is found to be unity which shows that the dominant mechanism for recombination is monomolecular type. A significant deviation from unity for the value for the scaling exponent could be expected when the mode of recombination changes from monomolecular to bimolecular recombination, particularly at higher light intensities. As a consequence of the linear variation of J_{SC} with P_{in} , it follows from Eq. (2) that V_{OC} should exhibit a slope of mkT/q , when plotted as a function of the logarithm of light intensity. The ideality factor of the inverted devices is found between 1.5 and 2.0.

This kink effect becomes dominant at higher temperature and/or intensity. In order to explore the origin of this kink, we examined the $J-V$ characteristic of the device by varying the light intensity and wavelengths. The kink feature persists at different wavelengths, indicating that the kink is not a result of the spatial distribution of the photogeneration rate, and under different light intensity, indicating that it is not due to charge trapping. The kink may however be due to the energy barrier at TiO_2 /fullerene or P3HT/Au interface.

4. CONCLUSION

We find that both temperature and illumination intensity slightly influence the power conversion efficiency of both conventional and inverted solar cells of P3HT:PCBM having a PEDOT:PSS layer. The fact that the power conversion efficiency of the inverted solar cells without PEDOT:PSS is increased over a factor of three within a

30 °C temperature increase is attributed to a consequence from the strong and positive temperature dependence of open-circuit voltage which may be due to a “kink” in the current–voltage characteristics near open-circuit voltage. However, the short-circuit current density and fill factor follows the same trend revealed by the conventional counterparts. We discussed the origin of this kink and how it can control the power conversion efficiency in the inverted devices.

Acknowledgment: P. Ravirajan and S. Sarithchandran thank the National Science Foundation, Sri Lanka for their financial assistance. Y. Kim thanks financial support from the Korean Government (National Research Foundation) grant (Priority Research Center Program_2009-0093819).

References and Notes

1. C. J. Brabec, N. S. Sariciftci, and J. C. Hummelen, *Adv. Funct. Mater.* 11, 15 (2001).
2. N. S. Sariciftci, L. Smilowitz, A. J. Heeger, and F. Wudl, *Science* 258, 1473 (1992).
3. I. Riedel, N. Martin, F. Giacalone, J. L. Segura, D. Chirvase, J. Parisi, and V. Dyakonov, *Thin Solid Film* 451, 48 (2004).
4. Y. Kim, S. A. Choulis, J. Nelson, D. D. C. Bradley, S. Cook, and J. R. Durrant, *Appl. Phys. Lett.* 86, 063502 (2005).
5. J. Y. Kim, S. H. Kim, H. Lee, K. Lee, W. Ma, X. Gong, and A. J. Heeger, *Adv. Mater.* 18, 572 (2006).
6. P. Ravirajan, S. A. Haque, D. Poplavskyy, J. R. Durrant, D. D. C. Bradley, and J. Nelson, *Thin Solid Film* 451, 624 (2004).
7. P. Ravirajan, S. A. Haque, J. R. Durrant, H. J. P. Smit, J. M. Kroon, D. D. C. Bradley, and J. Nelson, *Appl. Phys. Lett.* 86, 143101 (2005).
8. L. Kavan and M. Gratzel, *Electrochim. Acta* 40, 643 (1995).
9. P. Peumans and S. R. Forrest, *Appl. Phys. Lett.* 79, 126 (2001).
10. K. Takahashi, N. Kuraya, T. Yamaguchi, T. Komura, and K. Murata, *Sol. Energy Mater. Sol. Cells* 61, 403 (2000).
11. J. Nelson, J. Kirkpatrick, and P. Ravirajan, *Phys. Rev. B* 69, 035337 (2004).
12. J. Nelson, *The Physics of Solar Cells*, Imperial College Press, London (2003).
13. E. A. Katz, D. Faiman, S. M. Tuladhar, J. M. Kroon, M. M. Wienk, T. Fromherz, F. Padinger, C. J. Brabec, and N. S. Sariciftci, *J. Appl. Phys.* 90, 5343 (2001).
14. I. Riedel, J. Parisi, V. Dyakonov, L. Lutsen, D. Vanderzande, and J. C. Hummelen, *Adv. Funct. Mater.* 14, 38 (2004).
15. D. Chirvase, Z. Chiguvare, M. Knipper, J. Parisi, V. Dyakonov, and J. C. Hummelen, *J. Appl. Phys.* 93, 3376 (2003).

Received: 30 April 2010. Accepted: 16 June 2010.

JUNE 16, 2011

TRADE SERVICES

OUR REF. NO. : BTD/M035550

UNIVERSITY OF JAFFNA SRI LANKA
P O BOX 57
THIRUNELVELY, JAFFNA
SRI LANKA

Dear Sir;
OUR CREDIT NO : BTD/M035550 DATED JUNE 13, 2011
FOR 7,044.77 USD

We have debited your account No. 000000002026471 being charges on account of the above credit.


The charges recovered are detailed hereunder.

IMPORT LC COMMISSION	2,500.00 LKR
SWIFT CHARGES	2,500.00 LKR
VAT+NBT ON SWIFT CHARGES	357.00 LKR
TOTAL CHARGES	5,357.00 LKR

We have debited your Account No 000000002026471 for Margin in respect of above.

Margin Amount Debited 777,038.13 LKR 

Yours faithfully,

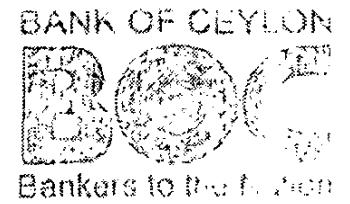

Manager (IMPORTS)
Bank of Ceylon

TAX INVOICE
VAT REGISTRATION NO. : 409000070-7000

Rs. 777,038.13 - 13/06/2011

(16)

SAB(S2)
CU



JUNE 16, 2011

TRADE SERVICES

OUR REF. NO. : BTD/M035550

UNIVERSITY OF JAFFNA SRI LANKA
P O BOX 57
THIRUNELVELY, JAFFNA
SRI LANKA

BRUNSON
K N N
TRADE SERVICES

Dear Sir;
OUR CREDIT NO : BTD/M035550 FOR 7,044.77 USD

We forward herewith copy of a Swift of the above credit which we established today in terms of your application. You are kindly requested to check this copy and advise us immediately in case of any errors or omissions. If no advice is received, it will be assumed that the terms of the credit conforms to your instructions

We have debited your account as per attached schedule.

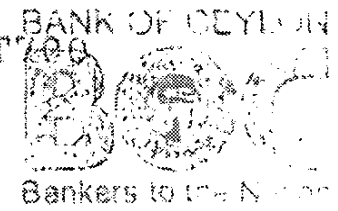
Further in terms of your instructions, we have made this Swift an operative credit instrument.

Yours faithfully,

Manager (IMPORTS)
Bank of Ceylon

DATE: JUN 16 2011

SWIFT MESSAGE - MT700



WELLS FARGO BANK N.A.
420 MONTGOMERY STREET
SAN FRANCISCO CALIFORNIA CA 94104
USA

{1:F01BCEYLKXLXAXXX0000000000}{2:I700WFBIUS6SXXX}TRADE SERVICES

:27: SEQUENCE OF TOTAL

1/1

:40A: FORM OF DOCUMENTARY CREDIT
IRREVOCABLE

:20: DOCUMENTARY CREDIT NUMBER
BTD/M035550

:31C: DATE OF ISSUE
110613

:40E: APPLICABLE RULES
UCP LATEST VERSION

:31D: DATE AND PLACE OF EXPIRY
110831U.S.A.

:51A: APPLICANT BANK
BCEYLKXLX

:50: APPLICANT
UNIVERSITY OF JAFFNA
JAFFNA

SRI LANKA

:59: BENEFICIARY
TERRA UNIVERSAL INC.
800, S. RAYMOND AVE, FULLERTON,
CA 92831,
U.S.A.

:32B: CURRENCY CODE, AMOUNT
USD7044,77

:39B: MAXIMUM CREDIT AMOUNT
NOT EXCEEDING

:41D: AVAILABLE WITH...BY...
ANY BANK IN U.S.A.

BY NEGOTIATION

:42C: DRAFTS AT
SIGHT

:42D: DRAWEE

BANK OF CEYLON
COLOMBO

:43P: PARTIAL SHIPMENTS
PARTIAL SHIPMENTS ARE PROHIBITED

:43T: TRANSHIPMENT
TRANSHIPMENTS ARE PROHIBITED

:44E: PORT OF LOADING /AIRPORT OF DEPARTURE
ANY PORT IN U.S.A.

:44F: PORT OF DISCHARGE/AIRPORT OF DESTINATION
COLOMBO, SRI LANKA

:44C: LATEST DATE OF SHIPMENT
110816

:45A: DESCRIPTION OF GOODS AND/OR SERVICES

LABORATORY EQUIPMENT (GLOVE BOX)

SHIPPING TERMS : EX-WORKS U.S.A.

H.S. NO(S) : 39.24.90.5500

:46A: DOCUMENTS REQUIRED

1. MANUALLY SIGNED COMMERCIAL INVOICE IN FOUR COPIES
SHOWING EX-WORKS VALUE QUOTING THE H S NUMBER AND CERTIFYING
THAT SHIPMENT IS IN CONFORMITY WITH APPLICANT'S ORDER
NO. S/P/02/2011 DATED 29/04/2011 AND CONFIRMATION
ORDER NO: 168430.

BANK OF CEYLON - TRADE SERVICES - CORPORATE BRANCH II

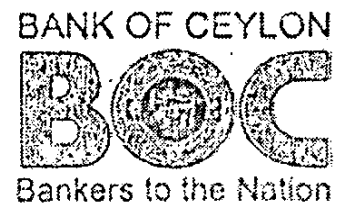
2nd Floor, Head Office, No. 4, Bank of Ceylon Mawatha, Colombo 01, Sri Lanka.

Imports - Tel: 94 11 2203242 to 50, 94 11 2446824, fax: 94 11 2542170 SWIFT: BCEYLKXLX, E-mail: sri@boc.lk

Exports - Tel: 94 11 2203280 to 99, 94 11 2541945, fax: 94 11 2445884, E-mail: cocxports@boc.lk Web: www.boc.lk

2. FULL SET OF CLEAN ON BOARD BILLS OF LADING

[Handwritten signatures]



TRADE SERVICES

22 JUN 2011

BANK OF CEYLON - TRADE SERVICES - CORPORATE BRANCH

2nd Floor, Head Office, No. 4, Bank of Ceylon Mawatha, Colombo 01, Sri Lanka.

Imports - Tel : 94 11 2203242 to 70 , 94 11 2446824, Fax : 94 11 2542170 SWIFT : BCEYLKX, E-mail : smg@bc.lk
Exports - Tel: 94112203280 to 99, 94112541945, Fax: 94112445334, E-mail: coexports@bc.lk Web: www.boc.lk

MADE OUT TO THE ORDER OF THE APPLICANT. FREIGHT PAYABLE AT DESTINATION. NOTIFY: APPLICANT. BANK OF CEYLON
3. CERTIFICATE OF U.S.A. ORIGIN (COMBINED CERTIFICATE OF ORIGIN AND INVOICE IS ACCEPTABLE).
4. PACKING LIST IN THREE COPIES.
5. CERTIFICATE FROM THE BENEFICIARY STATING THAT ONE COPY EACH OF THE DOCUMENTS CALLED FOR UNDER THE LETTER OF CREDIT HAS BEEN FACSIMILED DIRECT TO THE APPLICANT ON FAX NO: 94-21-2222644 AND THE SAME SET HAS BEEN DESPATCHED BY COURIER SERVICE DIRECT TO THE APPLICANT WITHIN SEVEN DAYS OF SHIPMENT.



Bankers to the Nation
TRADE SERVICES

:47A: ADDITIONAL CONDITIONS

1. TRANSPORT DOCUMENT(S) DATED PRIOR TO THE DATE OF THIS LETTER OF CREDIT NOT ACCEPTABLE.
2. INVOICE VALUE SHOULD NOT EXCEED THE VALUE AUTHORIZED BY THE LETTER OF CREDIT.
3. BILLS OF LADING TENDERED UNDER THIS LETTER OF CREDIT SHOULD BE ISSUED BY THE CEYLON SHIPPING CORPORATION LIMITED OR THEIR AUTHORISED AGENTS.
4. THE NEGOTIATING BANK MUST FORWARD ALL DOCUMENTS IN TWO LOTS, FIRST LOT BY COURIER SERVICE AND SECOND LOT BY AIR MAIL DIRECT TO THE MANAGER, BANK OF CEYLON, CORPORATE IMPORTS DEPARTMENT, NO.4, BANK OF CEYLON MAWATHA, COLOMBO 1, SRI LANKA.
5. THE NUMBER AND THE DATE OF THE LETTER OF CREDIT AND THE NAME OF OUR BANK MUST BE QUOTED ON ALL DRAFTS, INVOICES AND TRANSPORT DOCUMENTS REQUIRED.
6. NEGOTIATIONS MUST BE NOTED IN THE ORIGINAL LETTER OF CREDIT AND A NOTE TO THIS EFFECT SHOULD BE INDICATED ON COVERING LETTER.
7. A DISCREPANCY FEE OF USD 75.00 PLUS SWIFT CHARGES OR EQUIVALENT WILL BE DEDUCTED FROM EACH SET OF DOCUMENTS SUBMITTED WITH DISCREPANCIES.
8. UNLESS OTHERWISE STATED IN THE LETTER OF CREDIT. ALL DOCUMENT CONTENTS MUST BE IN ENGLISH.

:71B: CHARGES

ALL BANK CHARGES OUTSIDE SRI LANKA ARE FOR BENEFICIARYS ACCOUNT.

:48: PERIOD FOR PRESENTATION
DOCUMENTS MUST BE PRESENTED WITHIN 15 DAYS AFTER ISSUANCE OF THE TRANSPORT DOCUMENT BUT WITHIN THE VALIDITY OF THIS CREDIT

:49: CONFIRMATION INSTRUCTIONS WITHOUT

:78: INSTRUCTIONS TO THE PAYING/ACCEPTING/NEGOTIATING BANK ON RECEIPT OF DOCUMENTS AT OUR COUNTERS BEING IN STRICT COMPLIANCE WITH THE TERMS AND CONDITIONS OF THE LETTER OF CREDIT, WE SHALL REMIT PROCEEDS TO THE NEGOTIATING BANK AS PER INSTRUCTIONS TO BE RECEIVED.

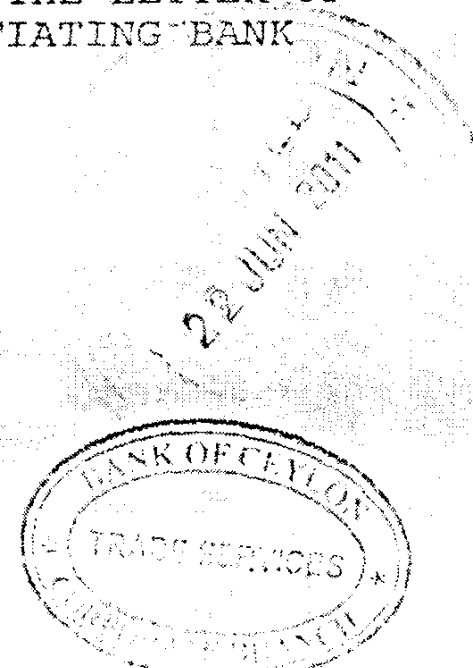
:57D: "ADVISE THROUGH" BANK
WELLS FARGO BANK

BUSINESS CENTER, 1661 N. RAYMOND
SUITE 102, ANAHEIM, CA.
U.S.A. 92801

:72: SENDER TO RECEIVER INFORMATION
IN CASE OF QUERIES, PLEASE CONTACT
US ON OUR HOTLINE 94-11-2338763.

- 1

Handwritten signatures



BANK OF CEYLON - TRADE SERVICES - CORPORATE BRANCH
2nd Floor, Head Office, No. 4, Bank of Ceylon Mawatha, Colombo 01, Sri Lanka.

Imports - Tel: 94 11 2203242 to 70, 94 11 2446824, Fax: 94 11 2542170 SWIFT: BCEYLK LX, E-mail: smcoim@boc.lk
Exports - Tel: 94 11 2203280 to 99, 94 11 2541945, Fax: 94 11 2446804, E-mail: coexports@boc.lk Web: www.boc.lk

Head / Physics

Equipment

UNIVERSITY OF JAFFNA, SRI LANK
THIRUNELVELY, JAFFNA.
SRI LANKA (CEYLON)


TERRA UNIVERSAL, Inc
800 S.Raymond Ave.,Fullerton
CA 92831
USA

Order No.: S/P/02/2011

Date: 29/04/2011

Please supply the undermentioned goods to the Head, Department of **Physics**, Univesity of Jaffna, Sri Lanka.

Item No.	Quantity	Description of Articles	Estimated Cost		Remarks or Reference to Specifications or Special Notice if/any/ B.T.N.Number
			Rate(USD \$)	Total(USD \$)	
01.	1	Glove Box,series 100,Acrylic,Single Model, 10" Port (Product No: 1689-00F)	1641.54	1,641.54	3924.90.5500
02.	1	Crating Charge (Product No: 1689-00D-9)	125	125.00	3924.90.5500
03.	1	Universal Air Lock;series 100,Acrylic (P.No:1680-80B)	400.51	400.51	3924.90.5500
04.	1	Changeable Sleeve & Glove: Size 9,for 10"- Diameter port,18" Sleev(P.No:1689-47)	279.28	279.28	3924.90.5500
05.	2	Automatic RB Valve;Installed,Polymer Glove Boxes & all Desiccators(P.No:1600--60B)	84.1	169.20	3924.90.5500
06.	1	Dual PurgeTM; for Glove box (P.No: 1603-57)	2,438.07	2,438.07	3924.90.5500
07.	1	Nitro Watch Controller (P.No:9500-00A)	777.67	777.67	3924.90.5500
08.	1	Nitro Watch / Humex Sensor (Installed) (P.No:9500-02A)	463.5	463.50	3924.90.5500
		L/C charges		750.00	
		Net Quote total		7,044.77	
		Total C.I.F (In USD \$)		7,044.77	


BORSAR 03/06/2011

Equivalent Sri Lanka Rs. 774,924.70

1. CERTIFICATE BY THE HEAD OF DEPARTMENT

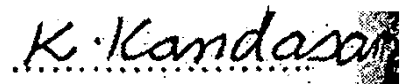
I hereby certify that the above articles are for educational and research purposes of the University of Jaffna, Sri Lanka.

Date:.


Head, Department of Physics

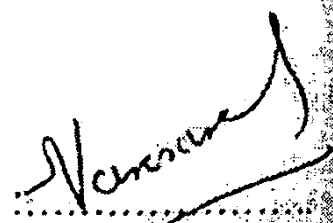
2. RECOMMENDATION BY THE DEAN

Date:.


Dean, Faculty of Science

3. APPROVAL OF THE VICE-CHANCELLOR

Date: 2011/06/08

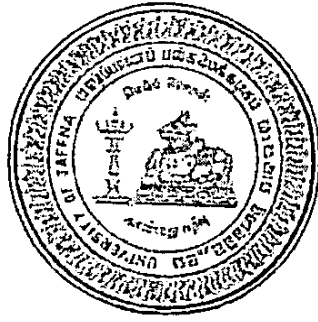

Vice-Chancellor
VICE CHANCELLOR
University of Jaffna
JAFFNA - SRI LANKA

UNIVERSITY OF JAFFNA, SRI LANKA
JAFFNA
SRI LANKA

මගේ අංකය }
எமது இல. }
My Number }

තැ.පෙ.අංකය-57
திரௌவேலி,
யாழ்ப்பாணம்

ඔබේ අංකය }
உமது இல. }
Your Number }



த.பெ. எண் - 57,
திரௌவேலி,
யாழ்ப்பாணம்.

දුරකථනය: 021-2222483
தொலைபேசி:021-2222006
Telephone : 021-2222644

යාපනය විශ්වවිද්‍යාලය, ශ්‍රී ලංකාව.
யாழ்ப்பாணப் பல்கலைக்கழகம், இலங்கை.
UNIVERSITY OF JAFFNA, SRI LANKA.

P.O. Box - 57,
Thirunelvely,
Jaffna.

Finance Branch

22.03.2012

Mrs. Rohini Wijeratne
Head / Research Foundation
National Science Division
47/5, Mantand Place
Colombo - 07

Submission of financial Report

RG/2007/FR/07

Dear Sir/ Madam,

This has referencē to your letter to Prof.P.Ravirajan Dept. of Physics University of Jaffna and copy to me dated 14/03/2012

We are sending herewith the Statement of Accounts from 04/04/2008 to 22/03/2012

Yours Sincerely,

.....
Bursar

CC: - Head Physics, University of Jaffna.

Chithra 22-03-2012

National Science Foundation

Grant No: RG/2007/FR/07

Statement of Accounts

Fund Received	
Year	Amount
2008	1,081,333.00
2009	360,000.00
2011	455,000.00
Total	1,896,333.00

* 67

Total Expenditure from 04/04/2008 to 22.03/2012

Personnel 898,333.33
Miscellaneous 2000.00
Total 900,333.33

+ Glove base. Expenses
refer
attachment

Balance available as at 22/03/2012 is Rs.995, 999.67

Pravin

Chh...

.....
Bursar
University Of Jaffna

National Digitization Project
National Science Foundation

Institute : National Science Foundation

1. Place of Scanning : Sanje (Private) Ltd, Hokandara

2. Date Scanned : 2017/04/18.....

3. Name of Digitizing Company : Sanje (Private) Ltd, No 435/16, Kottawa Rd,
Hokandara North, Arangala, Hokandara

4. Scanning Officer

Name : H.P.A.V. Caldera.....

Signature : H.P.A.V. Caldera.....

Certification of Scanning

I hereby certify that the scanning of this document was carried out under my supervision, according to the norms and standards of digital scanning accurately, also keeping with the originality of the original document to be accepted in a court of law.

Certifying Officer

Designation : Information Officer.....

Name : Renuka Sugathadasa.....

Signature : R. P. Sugathadasa.....

Date :

"This document/publication was digitized under National Digitization Project of the National Science Foundation, Sri Lanka"